

Reinforcement Learning for Node Selection in Branch-and-Bound

Anonymous authors
Paper under double-blind review

Abstract

A big challenge in branch and bound lies in identifying the optimal node within the search tree from which to proceed. Current state-of-the-art selectors utilize either hand-crafted ensembles that automatically switch between naive sub-node selectors, or learned node selectors that rely on individual node data. In contrast to existing approaches that only consider isolated nodes, we propose a novel simulation technique that uses reinforcement learning (RL) while considering the entire tree state. To achieve this, we train a graph neural network that produces a probability distribution based on the path from the model’s root to its “to-be-selected” leaves. Representing node-selection as a probability distribution allows us to train a decision-making policy using state-of-the-art RL techniques that capture both intrinsic node-quality and node-evaluation costs. Our method induces a high quality node selection policy on a set of varied and complex problem sets, despite only being trained on specially designed, synthetic travelling salesmen problem (TSP) instances. Using such a *fixed pretrained* policy shows significant improvements on several benchmarks in optimality gap reductions and per-node efficiency under **a short time limit of 45s and demonstrates generalization to a significantly longer 5min time limit.**

1 Introduction

The optimization paradigm of mixed integer programming plays a crucial role in addressing a wide range of complex problems, including scheduling (Bayliss et al., 2017), process planning (Floudas & Lin, 2005), and network design (Menon et al., 2013). A prominent algorithmic approach employed to solve these problems is *branch-and-bound (BnB)*, which recursively subdivides the original problem into smaller sub-problems through variable branching and pruning based on inferred problem bounds. BnB is also one of the main algorithms implemented in SCIP (Bestuzheva et al., 2021), a state-of-the art mixed integer linear and mixed integer nonlinear solver.

An often understudied aspect is the node selection problem, which involves determining which nodes within the search tree are most promising for further exploration. This is due to the intrinsic complexity of understanding the emergent effects of node selection on overall performance for human experts. Contemporary methods addressing the node selection problem typically adopt a per-node perspective (Yilmaz & Yorke-Smith, 2021; He et al., 2014; Morrison et al., 2016), incorporating varying levels of complexity and relying on imitation learning (IL) from existing heuristics (Yilmaz & Yorke-Smith, 2021; He et al., 2014). However, they fail to fully capture the rich structural information present within the branch-and-bound tree itself.

We propose a novel selection heuristic that leverages the power of bi-simulation: The BnB tree-structure and its expansion/pruning dynamics are directly replicated inside our neural network model. We now employ reinforcement learning (RL) to learn a heuristic that is naturally well aligned to the branch-and-bound problem, see Fig. 1. The resulting method is able to take advantage of the inherent structure inside the branch-and-bound algorithm which leads to superior generalization compared to the seminal work by Labassi et al. (2022). This allows the RL policy to directly account for the BnB tree’s dynamics.

We reason that RL specifically is a good fit for this type of training as external parameters outside the pure quality of a node have to be taken into account. For example, a node A might promise a significantly

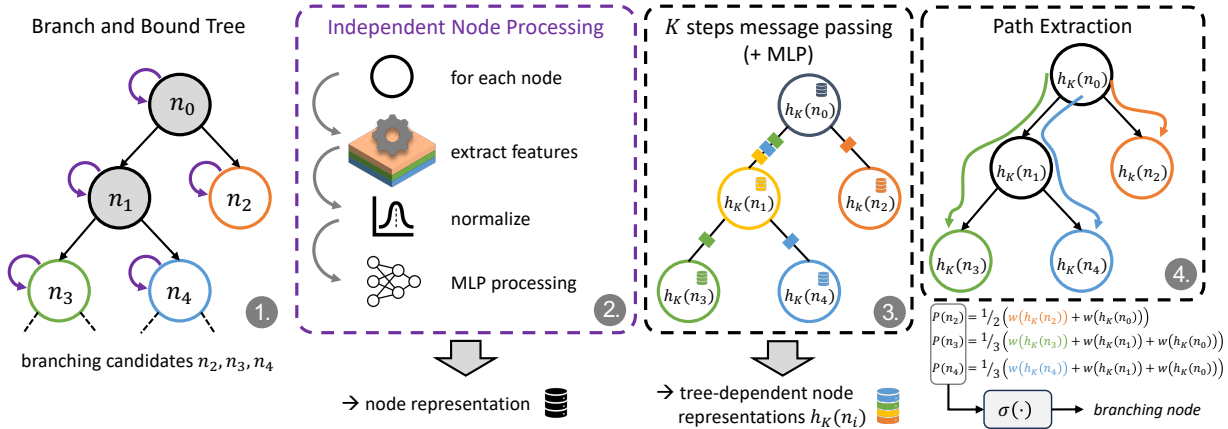


Figure 1: **Overview of our approach:** (1) SCIP solves individual nodes and executes existing heuristics. (2) Features are extracted from every branch-and-bound node and sent to individual normalization and embedding. (3) The node embeddings are subject to K steps of GNN message passing on the induced tree-structure. **The embeddings are projected to scalar weights and values using a Multi Layer Perceptron (MLP).** (4) Based on the node embeddings, we generate root-to-leaf paths, from which we sample the next node. The resulting node is submitted to SCIP and we return to step 1.

bigger decrease in the expected optimality gap than a second node B , but node A might take twice as long to evaluate, making B the “correct” choice despite its lower theoretical utility. By incorporating the bi-simulation technique, we can effectively capture and propagate relevant information throughout the tree.

The main contributions of this paper are:

- a method for processing branch-and-bound trees of arbitrary size, which probabilistically samples leaves of the BnB tree by modeling the selection as a root-to-leaf traversal of the BnB tree,
- a new way of sampling optimization instances of intermediary difficulty,
- a thorough time-limited benchmark on industrial-scale instances contained in TSPLIB, MINLPLib, and MIPLIB, and
- an analysis of the learned node selector using explainable-AI techniques

To the best of our knowledge we are the first to present a learned selection method that now only generalizes across instance types but that also is applicable to nonlinear mixed-integer optimization.

The rest of this article is structured as follows. Sec. 2 describes branch and bound and Sec. 3 discusses related work. Sec. 4 explains our method, i.e., our node representation, our node selection agent, and how we generate training instances. Sec. 5 discusses the experiments and Sec. 6 discusses limitations. Sec. 7 concludes.

2 Branch and Bound

BnB is one of the most effective methods for solving mixed integer programming (MIP) problems. It recursively solves relaxed versions of the original problem, gradually strengthening the constraints until it finds an optimal solution. The first step relaxes the original MIP instance into a tractable subproblem by dropping all integrality constraints such that the subproblem can later be strictified into a MIP solution. For simplicity, we focus our explanation to the case of mixed integer linear programs (MILP) while our method theoretically works for any type of constraint allowed in SCIP (see nonlinear results in Sec. 5.3.1, and Bestuzheva et al. (2023)). Concretely a MILP has the form

$$P_{\text{MILP}} = \min\{c_1^T x + c_2^T y \mid Ax + By \geq b, y \in \mathbb{Z}^n\}, \quad (1)$$

where c_1 and c_2 are coefficient vectors, A and B are constraint matrices, and x and y are variable vectors. The integrality constraint $y \in \mathbb{Z}^n$ requires y to be an integer. In the relaxation step, this constraint is dropped,

leading to the following simplified problem:

$$P_{\text{relaxed}} = \min\{c_1^T x + c_2^T y \mid Ax + By \geq b\}. \quad (2)$$

Now, the problem becomes a linear program without integrality constraints, which can be exactly solved using the Simplex (Dantzig, 1982) or other efficient linear programming algorithms.

After solving the relaxed problem, BnB proceeds to the branching step: First, a non-integral y_i is chosen. The branching step then derives two problems: The first problem (Eq. 3) adds a lower bound to variable y_i , while the second problem (Eq. 4) adds an upper bound to variable y_i . These two directions represent the rounding choices to enforce integrality for y_i :¹

$$P_{\text{relaxed}}^1 = \min\{c_1^T x + c_2^T y \mid Ax + By \geq b, y_i \leq \lfloor c \rfloor\} \quad (3)$$

$$P_{\text{relaxed}}^2 = \min\{c_1^T x + c_2^T y \mid Ax + By \geq b, y_i \geq \lceil c \rceil\} \quad (4)$$

The resulting decision tree, with two nodes representing the derived problems can now be processed recursively. However, a naive recursive approach exhaustively enumerates all integral vertices, leading to an impractical computational effort. Hence, in the bounding step, nodes that are deemed worse than the currently known best solution are discarded. To do this, BnB stores previously found solutions which can be used as a lower bound to possible solutions. If a node has a **lower** bound larger than a currently found integral solution, no node in that subtree has to be processed.

The interplay of these three steps—relaxation, branching, and bounding—forms the core of branch-and-bound. It enables the systematic exploration of the solution space while efficiently pruning unpromising regions. Through this iterative process, the algorithm converges towards the globally optimal solution for the original MIP problem, while producing optimality bounds at every iteration.

3 Related Work

Learning node selection, where learned heuristics pick the best node to continue from the search tree, has only rarely been addressed in research. Prior work that learns such node selection strategies made significant contributions to improve the efficiency and effectiveness of the optimization.

Notably, many approaches rely on per-node features and Imitation Learning (IL). Otten & Dechter (2012) **study** the estimation of subproblem complexity as a means to enhance parallelization efficiency. By estimating the complexity of subproblems, the algorithm can allocate computational resources of parallel solvers more effectively. Yilmaz & Yorke-Smith (2021) **employ** IL to directly select the most promising node for exploration. Their approach **utilizes** a set of per-node features to train a model that can accurately determine which node to choose. He et al. (2014) **make us of** support vector machines and IL to create a hybrid heuristic based on existing heuristics. By leveraging per-node features, their approach **aims** to improve node selection decisions. While these prior approaches **yield** valuable insights, they are inherently limited by their focus on per-node features.

Labassi et al. (2022) **propose** the use of Siamese graph neural networks, representing each node as a graph that connects variables with the relevant constraints. Their objective **is to directly imitate** an optimal diving oracle, **which descends depth-first towards a node containing a minimal value**. This approach **facilitates** learning from node comparisons and **enables** the model to make informed decisions during node selection. This means that Labassi et al. (2022) manages to study pairs of leaf-subproblems, rather than studying every subproblem in isolation. However, this method still does not utilize the high information content given by the tree structure itself: The search tree itself slowly gathers information in the form of, e.g., cutting planes or the optimality of solutions close to (but not inside) the current subproblem’s feasible set.

Aside of the work in learning node selection, there **is also** substantial work in learning different heuristics for branch and bound. One commonly learned component of branch and bound is the *variable selection* heuristic (Scavuzzo et al., 2022; Parsonson et al., 2022; Gasse et al., 2019; Etheve et al., 2020). Variable

¹There are non-binary, “wide” branching strategies which we will not consider here explicitly. However, our approach is flexible enough to allow for arbitrary branching width. See Morrison et al. (2016) for an overview.

selection is the problem of which variable to apply the branch for the subproblems, i.e., which y_i to add a constraint to in Eqs 3 and 4. **Other frequently learned heuristics include *cut-selection methods*** (Tang et al., 2019; Wang et al., 2023; Paulus et al., 2022; Turner et al., 2022). Cut selection is part of an extension of branch-and-bound known as branch-and-cut, which additionally adds constraints to sub-problems **that remove solutions that are feasible in a node’s linear relaxation, but are infeasible in the original MILP model.** Specifically, if x is a solution to the relaxed Equation 2, but not a solution to the MILP Equation 1, a new constraint is placed into the relaxation that removes the found x from the problem. Such cuts are generally **not unique**. Cut selection is the process of picking the best cuts from a set of different feasible cuts. *However, all these (types of) heuristics are orthogonal to our node selection problem: One can apply both our learned node selector as well as any combination of cut and variable selectors.*

Compared to both cut and variable selection, node selection is severely under-researched due to its inherent complexity. While both variable selection and cut selection can be solved by studying a single sub-problem in isolation, node selection has to study the set of all possible sub-problems as a whole, which increases the complexity of building node selectors.

4 Methodology

We model the node selection process as a sequential Markov Decision Process (MDP). An MDP consists of a set of observable states $s \in \mathcal{S}$, a set of controllable actions $a \in \mathcal{A}$, a reward function $R(s)$ describing the quality of an individual state $s \in \mathcal{S}$ in isolation, and a (typically unknown) transition distribution $T : \mathcal{S} \times \mathcal{A} \rightarrow \mathcal{S}$ that takes in a current state $s \in \mathcal{S}$ and an action $a \in \mathcal{A}$, proposed by a decision-making policy $\pi : \mathcal{S} \rightarrow \mathcal{A}$, and produces a distribution over new state $s' \in \mathcal{S}$. The policy is usually thought of as a conditional distribution $\pi(a|s)$ producing the next action $a \in \mathcal{A}$ under the knowledge of the current state $s \in \mathcal{S}$. Our objective is to find the policy optimal π^* , which maximizes the expected discounted sum of future rewards:

$$\pi^* = \operatorname{argmax}_{\pi} \mathbb{E} \left[\sum_{t=0}^{t_{\max}} \gamma^t R(s_t) \pi(a_t|s_t) T(s_{t+1}|s_t, a_t) \right], \quad (5)$$

where $0 < \gamma < 1$ is a factor to trade immediate over future rewards (Sutton & Barto, 2018).

RL is the process of solving such MDPs by repeatedly rolling out π on an environment and using the resulting trajectories to find a policy π that maximizes the return. Several solvers for MDPs exist, such as Deep Q-Networks (DQN) (Mnih et al., 2015) or Proximal Policy Optimization (PPO) (Schulman et al., 2017). In this paper we use PPO to solve the MDP.

In our case, we phrase our optimization problem as an MDP, where states s_t are represented using directed branch-and-bound trees, actions a_t are all selectable leaf-nodes, and the reward R is set according to Eq. 6 in Sec. 4.1. The transitions are given by the SCIP-solver and its heuristics: Given the current state (BnB tree) and the node selection by π , the SCIP solver produces new nodes as children of the selected ones, and prunes unnecessary nodes from the tree. To solve the MDP, PPO needs a representation for the policy π and a model describing the state-value-function, defined as $V(s) = \max_a Q(s_t, a)$ (see Schulman et al. (2017)).

In our model, we represent the branch-and-bound tree as a directed Graph Neural Network (GNN) whose nodes and edges are in an 1:1 correspondence to the branch-and-bound nodes and edges, see Sec. 4.2. This means that for every node in the BnB tree there is exactly one node in the GNN, and every connection in the BnB tree is replicated in the GNN graph. As the BnB tree grows, the GNN graph grows as well, solving one of the biggest issues in node selection: Since the BnB tree grows and shrinks dynamically, the number of different node selections (= actions) changes drastically. One benefit of our GNN model is that the resulting directed graph automatically grows/shrinks the action space as new nodes are added/pruned from the tree since the policy’s action-space directly corresponds to the leaves of the GNN/BnB tree. This allows our network to phrase node selection explicitly as a distribution over node-selections, rather than using implicit comparisons as in Labassi et al. (2022).

4.1 Reward Definition

A common issue in MIP training is the lack of good reward functions. For instance, the primal-dual integral used in Gasse et al. (2022) has the issue of depending on the scale of the objective, needing a primally feasible solution at the root, and being very brittle if different instance difficulties exist in the instance pool. Gasse et al. (2022) circumvents these issues by generating similar instances, while also supplying a feasible solution at the root. However, to increase generality, we do not want to make as strict assumptions as having similar instance difficulties, introducing a need for a new reward function. A reasonable reward measure captures the achieved performance against a well-known baseline. In our case, we choose our reward, to be

$$r = - \left(\frac{\text{gap}(\text{Node Selector})}{\text{gap}(\text{SCIP})} - 1 \right), \quad (6)$$

where $\text{gap}(\text{SCIP})$ denotes the optimality gap reachable by the standard SCIP node selector in the set time limit (for us 45s), and $\text{gap}(\text{node selector})$ denotes the gap reachable by our method within the set time limit. This represents the relative performance of our selector compared to the performance achieved by SCIP.

Intuitively, the aim of this reward function is to decrease the optimality gap achieved by our node-selector (i.e., $\text{gap}(\text{node selector})$), normalized by the results achieved by the existing state-of-the-art node-selection methods in the SCIP (Bestuzheva et al., 2021) solver (i.e., $\text{gap}(\text{SCIP})$). This accounts for varying instance hardness in the dataset. Further, we shift this performance measure, such that any value > 0 corresponds to our selector being superior to existing solvers, while a value < 0 corresponds to our selector being worse, and clip the reward between $(1, -1)$ to ensure symmetry around zero as is commonly done in prior work (see, e.g. Mnih et al. (2015); Dayal et al. (2022)). This formulation has the advantage of looking at relative improvements over a baseline, rather than absolute performance, which allows us to use instances of varying complexity during training.

We also experimented with other metrics that aim to normalize for the complexity of the instance themselves (see Appendix C). We found that the reward metric as proposed here is the most stable to train and yields the best results w.r.t. minimizing the optimality gap.

4.2 Tree Representation

To represent the MDP’s state, we propose a novel approach that involves bi-simulating the existing branch-and-bound tree using a graph neural network (GNN). Specifically, we consider the state to be a directed tree $T = (V, E)$, where V are individual subproblems created by SCIP, and E are edges set according to SCIP’s node-expansion rules. More precisely, the tree’s root is the principle relaxation (Eq. 2), and its children are the two rounding choices (Eqs. 3 and 4). BnB proceeds to recursively split nodes, adding the splits as children to the node it was split from.

For processing inside the neural network, we extract features (see Appendix A) from each node, keeping the structure intact: $T = (\text{extract}(V), E)$. We ensure that the features stay at a constant size, independent from, e.g., the number of variables and constraints, to enable efficient batch-evaluation of the entire tree.

For processing the tree T , we use message-passing from the children to the parent. Pruned or missing nodes are replaced with a constant to maintain uniformity over the graph structure. Message-passing enables us to consider the depth- K subtree under every node by running K steps of message passing from the children to the parent. Concretely, the internal representation can be thought of initializing $h_0(n) = x(n)$ (with $x(n)$ being the features associated with node n) and then running K iterations jointly for all nodes n :

$$h_{t+1}(n) = h_t(n) + \text{emb} \left(\frac{h_t(\text{left}(n)) + h_t(\text{right}(n))}{2} \right), \quad (7)$$

where $\text{left}(n)$ and $\text{right}(n)$ are the left and right children of n , respectively, $h_t(n)$ is the hidden representation of node n after t steps of message passing, and emb is a function that takes the mean hidden state of all embeddings and creates an updated node embedding. Doing this for K steps aggregates the information of the depth- K limited subtree of n into the node n .

4.3 RL for Node Selection

While the GNN model is appealing, it is impossible to train using contemporary imitation learning techniques, as the expert’s action domain (i.e., leaves) may not be the same as the policy’s action domain, meaning that the divergence between these policies is undefined.

To solve this problem, we choose to use model-free reinforcement learning techniques to directly maximize the probability of choosing the correct node. State-of-the-art reinforcement learning techniques, such as proximal policy optimization (PPO) (Schulman et al., 2017), need to be able to compute two functions: The value function $V(s) = \max_{a \in \mathcal{A}} Q(s, a)$, and the likelihood function $\pi(a|s)$. **PPO uses the value function to reduce the variance of the advantage computation. In our work, we utilize the Generalized Advantage Estimator (GAE) Schulman et al. (2015) which provides a continuous mixture of bootstrapped and Monte Carlo estimated advantages.** As it turns out, there are efficient ways to compute both of these values from a tree representation:

Firstly, we can produce a probability distribution of node-selections (i.e., our actions) by computing the expected “weight” across the unique path from the graph’s root to the “to-be-selected” leaves. These weights are mathematically equivalent to the unnormalized log-probabilities of choosing a leaf-node by recursively choosing either the right or left child with probability p and $1 - p$ respectively. The full derivation of this can be found in Appendix B. Concretely, let n be a leaf node in the set of choosable nodes \mathcal{C} , also let $P(r, n)$ be the unique path from the root r to the candidate leaf node, with $|P(r, n)|$ describing its length. We define the expected path weight $W'(n)$ to a leaf node $n \in \mathcal{C}$ as

$$W'(n) = \frac{1}{|P(r, n)|} \sum_{u \in P(r, n)} W(h_K(u)). \quad (8)$$

Selection now is performed in accordance to sampling from a selection policy π induced by

$$\pi(n | \text{tree}) = \text{softmax}(\{W'(n) | \forall n \in \mathcal{C}\}). \quad (9)$$

Intuitively, this means that we select a node exactly if the expected utility along its path is high. Note that this definition is naturally self-correcting as erroneous over-selection of one subtree will lead to that tree being completed, which removes the leaves from the selection pool \mathcal{C} .

Similar to the log-likelihood, we parameterize the value function as a root-to-leaf sum, which is aggregated using a $\max(\cdot)$ over paths.

$$f(n|s) = \frac{\tilde{f}(n|s)}{|P(r, n)|} \quad (10)$$

$$\tilde{f}(n|s) = \tilde{f}(\text{left}|s) + \tilde{f}(\text{right}|s) + f(h_K(n)|s) \quad (11)$$

$$V(s) = \max \{f(n) \mid \forall n \in \mathcal{C}\}, \quad (12)$$

where $f(h_n)$ is a trained per-node estimator, \hat{f} is the path-aggregated f -function, and \mathcal{C} is the set of open nodes as proposed by the branch-and-bound method. **For an alternative parametrization of $V(\cdot)$ that justifies the use of \tilde{f} as a Q-function, see Appendix J.** Since we can compute the action likelihood $\pi(a|s)$, the value function $V(s)$, and the Q-function $Q(s, a)$, we can use any Actor-Critic method (like PPO (Schulman et al., 2017) or A3C (Mnih et al., 2016)) for training this model. We **use** PPO due to its ease of use and robustness.

According to these definitions, we only need to predict the node embeddings for each node $h_K(n)$, the per-node q-function $q(h_K(n)|s)$, and the weight of each node $W(h_K(u))$. We parameterize all of these as MLPs (more architectural details can be found in Appendix E).

This method provides low, but measurable overhead compared to existing node selectors, even if we discount the fact that our Python-based implementation is vastly slower than SCIP’s highly optimized C-based implementation. Hence, we focus our model on being efficient at the beginning of the selection process, where good node selections are exponentially more important as finding more optimal solutions earlier allows to prune more nodes from the exponentially expanding search tree. Specifically we evaluate our heuristic at

every node for the first 250 selections, then at every tenth node for the next 750 nodes, and finally switch to classical selectors for the remaining nodes.²

4.4 Data Generation & Agent Training

In training MIPs, a critical challenge lies in generating sufficiently complex training problems. First, to learn from interesting structures, we need to decide on some specific problem, whose e.g. satisfiability is knowable as generating random constraint matrices will likely generate empty polyhedrons, or polyhedrons with many eliminable constraints (e.g., in the constraint set consisting of $c^T x \leq b$ and $c^T x \leq b + \rho$ with $\rho \neq 0$ one constraint is always eliminable). This may seem unlikely, but notice how we can construct aligned c vectors by linearly combining different rows (just like in LP-dual formulations). In practice, selecting a sufficiently large class of problems may be enough as during the branch-and-cut process many sub-problems of different characteristics are generated. Since our algorithm naturally decomposes the problem into sub-trees, we can assume any policy that performs well on the entire tree also performs well on sub-polyhedra generated during the branch-and-cut.

For this reason we consider the large class of Traveling Salesman Problem (TSP), which itself has rich use-cases in planning and logistics, but also in optimal control, the manufacturing of microchips and DNA sequencing (see Cook et al. (2011)). The TSP problem consists of finding a round-trip path in a weighted graph, such that every vertex is visited exactly once, and the total path-length is minimal (for more details and a mathematical formulation, see Appendix F).

For training, we would like to use random instances of TSP but generating them can be challenging. Random sampling of distance matrices often results in easy problem instances, which do not challenge the solver. Consequently, significant effort is being devoted into devising methods for generating random but hard instances, particularly for problems like the TSP, where specific generators for challenging problems have been designed (see Vercesi et al. (2023) and Rardin et al. (1993)). However, for our specific use cases, these provably hard problems may not be very informative as they rarely contain efficiently selectable nodes.

To generate these intermediary-difficult problems, we adopt a multi-step approach: We begin by generating random instances and then apply some mutation techniques (Bossek et al., 2019) to introduce variations, and ensure diversity within the problem set. Next, we select the instance of median-optimality gap from the pool, which produces an instance of typical difficulty. The optimality gap, representing the best normalized difference between the lower and upper bound for a solution found during the solver’s budget-restricted execution, serves as a crucial metric to assess difficulty. This method is used to produce 200 intermediary-difficult training instances.

To ensure the quality of candidate problems, we exclude problems with more than 100% or zero optimality gap, as these scenarios present challenges in reward assignment during RL. To reduce overall variance of our training, we limit the ground-truth variance in optimality gap. Additionally, we impose a constraint on the minimum number of nodes in the problems, discarding every instance with less than 100 nodes. This is essential as we do not expect such small problems to give clean reward signals to the reinforcement learner.

5 Experiments

For our experiments we consider the instances of TSPLIB (Reinelt, 1991) and MIPLIB (Gleixner et al., 2021) which are one of the most used datasets for benchmarking MIP frameworks and thusly form a strong baseline to test against. We further test against the UFLP instance generator by (Kochetov & Ivanenko, 2005), which specifically produces instances hard to solve for branch-and-bound, and against MINLPLIB (Bussieck et al., 2003), which contains *mixed integer nonlinear programs*, to show generalization to **vastly** different problems.

We perform all our training and the experiments on a Ryzen 7 5800x3d CPU, where training completes after approx. 6h. After the model is trained on the synthetic TSP instances, we freeze the network and apply it to

²This accounts for the “phase-transition” in MIP solvers where optimality needs to be proved by closing the remaining branches although the theoretically optimal point is already found (Morrison et al., 2016). Note that with a tuned implementation we could run our method for more nodes, where we expect further improvements.

both the “in distribution” TSPLIB and the “out of distribution” UFLP, MINLPLIB and MIPLIB instances. This is in contrast to prior work such as those from Labassi et al. (2022), who train separate models for all instance types and do not manage to generalize to foreign instances (see Sec 5.4). Our source code is publicly available and can be used to reproduce the experiments.³ We use the default hyperparameters as proposed by CleanRL (Huang et al., 2021).

For our benchmarks on TSPLIB, UFLP, MIPLIB and MINLPLIB, we impose a time limit of 45s and 5min. We report the expected reward (Eq. 6), the geometric mean of the achieved gap for both our and the baseline method, and the win-rate of our method as defined by $\text{gap}(\textit{ours}) \leq \text{gap}(\textit{baseline})$.⁴ For longer runs with a timelimit of 30min see Appendix D.

5.1 Baselines

We run both our method and SCIP for 45s. We then filter out all runs where SCIP has managed to explore less than 5 nodes, as in these runs even perfect node selection makes no difference in performance. If we included those in our average, we would have a significant number of lines where our node-selector has zero advantage over the traditional SCIP one, not because our selector is better or worse than SCIP, but simply because it wasn’t called in the first place. We set this time-limit relatively low as our prototype selector only runs at the beginning of the solver process, meaning that over time the effects of the traditional solver take over.

Additionally, we also consider an evaluation with a 5min time limit. For those runs, the limit until we switch to the naive node selector is set to 650 nodes to account for the higher time limit. In general, the relative performance of our method compared to the baseline increases with the 5min budget.

Finally, we also benchmark against the previous state-of-the-art by Labassi et al. (2022), which represents optimal node selection as a comparison problem where a siamese network is used to compare different leaf nodes against each other and picking the “highest” node as the next selection.

5.2 Results

While all results can be found in Appendix I we report an aggregated view for each benchmark in Table 1. In addition to our “reward” metric we report the winning ratio of our method over the baseline, and the geometric mean of the gaps at the end of solving (lower is better).

For benchmarking and training, we leave all settings, such as presolvers, primal heuristics, diving heuristics, constraint specializations, etc. at their default settings to allow the baseline to perform best. All instances are solved using the same model without any fine-tuning. We expect that tuning, e.g., the aggressiveness of primal heuristics, increases the performance of our method, as it decreases the relative cost of evaluating a neural network, but for the sake of comparison we use the default parameters for all our tests. We train our node selection policy on problem instances according to Sec. 4.4 and apply it on problems from different benchmarks.

First, we will discuss TSPLIB itself, which while dramatically more complex than our selected training instances, still contains instances from the same problem family as the training set (Sec. 5.2.1). Second, we consider instances of the Uncapacitated Facility Location Problem (UFLP) as generated by Kochetov & Ivanenko (2005)’s problem generator. These problems are designed to be particularly challenging to branch-and-bound solvers due to their large optimality gap (Sec. I.1). While the first two benchmarks focused

³Source code: a link to the public repository will be made available upon acceptance.

⁴All of these metrics give a slightly different view of the performance of our method: The **reward** metric is naturally balanced to weight the improvement relative to the difficulty of the problem as reward captures the improvement over the baseline in percent (higher is better). The downside of this is that because reward is balanced, it will assign the same reward to an improvement of $5\text{gap} \rightarrow 2.5\text{gap}$ as to $0.5\text{gap} \rightarrow 0.25\text{gap}$, which can overemphasize the impact of easy to solve instances. **Win-rate** is a supplementary metric showing the percentage of instances where our model *beats the baseline*. This can help show how the improvements are distributed among the instances (higher is better). Finally, comparing the **geometric mean** is the gold-standard tool in measuring solver performance (Bestuzheva et al., 2021). In contrast to the reward metric, geometric means are specifically designed to reject outliers increasing the robustness of the metric. We report both our geometric mean and the SCIP baseline’s geometric mean (our $\text{gap} < \text{SCIP gap}$ is better).

Table 1: Performance across benchmarks (the policy only saw TSP instances during training). The reward is the normalized improvement over the baseline (Eq. 6) averaged over the benchmarking dataset, the win-rate shows how often our method produces a better (or in case of both methods reaching 0% gap equal) optimality gap, and the geometric means are the shifted geometric means of optimality gaps computed over the benchmarking dataset

Benchmark	Reward	Win-rate	geo-mean Ours	geo-mean SCIP
TSPLIB (Reinelt, 1991)	0.184 \pm 0.52	0.50	0.931	0.957
UFLP (Kochetov & Ivanenko, 2005)	0.078 \pm 0.19	0.636	0.491	0.520
MINLPLib (Bussieck et al., 2003)	0.487 \pm 0.60	0.852	28.783	31.185
MIPLIB (Gleixner et al., 2021)	0.140 \pm 0.69	0.769	545.879	848.628
TSPLIB@5min	0.192 \pm 0.51	0.600	1.615	2.000
MINLPLib@5min	0.486 \pm 0.60	0.840	17.409	20.460
MIPLIB@5min	0.150 \pm 0.69	0.671	66.861	106.400

on specific problems (giving you a notion of how well the algorithm does on the problem itself) we next consider “meta-benchmarks” that consist of many different problems, but relatively few instances of each. MINLPLIB (Bussieck et al., 2003) is a meta-benchmark for *nonlinear* mixed-integer programming (Sec. 5.3.1), and MIPLIB (Gleixner et al., 2021) a benchmark for mixed integer programming (Sec. 5.3.2). We also consider generalization against the uncapacitated facility location problem using a strong instance generator, see Appendix I.1. Our benchmarks are diverse and complex and allow to compare algorithmic improvements in state-of-the-art solvers.

5.2.1 TSPLIB

From an aggregative viewpoint we outperform the SCIP node selection by $\approx 20\%$ in reward. However, the overall “win-rate” is only 50% as the mean-reward is dominated by instances where our solver has significant performance improvements: When our method loses, it loses by relatively little (e.g., `att48`: ours 0.287 vs base 0.286), while when it wins, it usually does so by a larger margin.

Qualitatively, it is particularly interesting to study the problems our method still loses significantly against SCIP (in four cases). A possible reason why our method significantly underperforms on `Dantzig42` is that our implementation is just too slow, considering that the baseline manages to evaluate $\approx 40\%$ more nodes. A similar observation can be made on `eil51` where the baseline manages to complete $5\times$ more nodes. `rd100` is also similar to `Dantzig` and `eil51` as the baseline is able to explore 60% more nodes. `KroE100` is the first instance our method loses against SCIP, despite exploring a roughly equal amount of nodes. We believe that this is because our method commits to the wrong subtree early and never manages to correct into the proper subtree. Ignoring these four failure cases, our method is either on par (up to stochasticity of the algorithm) or exceeds the baseline significantly.

It is also worthwhile to study the cases where both the baseline and our method hit 0 optimality gap. Both algorithms reaching zero optimality gap can be seen as somewhat of a special case, since solely looking at the solution value is insufficient to figure out which method performs better in practice. A quick glance at instances like `bayg29`, `fri26`, `swiss42` or `ulysses16` shows that our method tends to finish these problems with significantly fewer nodes explored. This is not captured by any of our metrics since those only look at solution quality, not the efficiency of reaching that solution. If the quality of the baseline and ours is the same, it makes sense to look at solution efficiency instead. Qualitatively, instances like `bayg29` manage to reach the optimum in only $\frac{1}{3}$ the number of explored nodes, which showcases a significant improvement in node-selection quality. It is worth noting that, due to the different optimization costs for different nodes, it is not always true that evaluating fewer nodes is faster in wall-clock time. In practice, “fewer nodes is better” seems to be a good rule-of-thumb to check algorithmic efficiency.

5.3 UFLP

The UFLP benchmark designed by Kochetov & Ivanenko (2005) is specifically built to be hard to solve by branch-and-bound solvers due to its large duality gap. Despite this, our method manages to outperform the baseline significantly. This is meaningful since this benchmark is a specially designed worst-case scenario: The fact that our method still outperforms the baseline provides good evidence of the efficacy of the method.

5.3.1 MINLPLIB

We now consider MINLPs. To solve these, SCIP and other solvers use branching techniques that cut nonlinear (often convex) problems from a relaxed master-relaxation towards true solutions. We consider MINLPLib (Bussieck et al., 2003), a meta-benchmark consisting of hundreds of diverse synthetic and real-world MINLP instances of varying different types and sizes. As some instances take hours to solve even a single node, we filter out all problems with fewer than 5 nodes, as the performance in those cases is independent of the node-selectors performance (Full results Appendix I.4).

Our method still manages to outperform SCIP, even on MINLPs, despite never having seen a single MINLP problem before, see Table 1. Qualitatively, our method either outperforms or is on par with the vast majority of problems, but also loses significantly in some problems, greatly decreasing the average. Studying the cases our method loses convincingly (see Appendix I.4), we find a similar case as in TSPLIB, where the baseline implementation is so much more optimized that significantly more nodes can get explored. We suspect the reason our method has the biggest relative improvements on MINLPs is due to the fact that existing e.g. pseudocost based selection methods do not perform as well on spatial-branch-and-bound tasks.

We expect features specifically tuned for nonlinear problems to increase performance by additional percentage points, but as feature selection is orthogonal to the actual algorithm design, we leave more thorough discussion of this to future work ⁵.

5.3.2 MIPLIB

Last, but not least we consider the meta-benchmark MIPLIB (Gleixner et al., 2021), which consists of hundreds of real-world mixed-integer programming problems of varying size, complexity, and hardness. Our method is either close to or exceeds the performance of SCIP, see Table 1.

Considering per-instance results, we see similar patterns as in previous failure cases: Often we underperform on instances that need to close many nodes, as our method’s throughput lacks behind that of SCIP. We expect that a more efficient implementation alleviates the issues in those cases.

We also see challenges in problems that are far from the training distribution, specifically satisfaction problems. Consider `fnw-binpack4-48`, where the baseline yields an optimality gap of 0 while we end at $+\infty$. This is due to the design of the problem: Instead of a classical optimization problem, this is a satisfaction problem, where not an optimal value, but *any* feasible value is searched, i.e., we either yield a gap of 0 (solution found), or a gap of $+\infty$ (solution not found), as no other gap is possible. Notably, these kinds of problems may pose a challenge for our algorithm, as the node-pruning dynamics of satisfying MIPs are different than the one for optimizing MIPs: Satisfying MIPs can only rarely prune nodes since, by definition, no intermediary primarily valid solutions are ever found.

5.4 Comparison against “Learning to compare nodes”

Aside from comparisons against SCIP, we also compare against the previous state-of-the-art method by Labassi et al. (2022). One complication when benchmarking against Labassi et al. (2022) is that they assume a *separate model for each problem type*, while our method is already flexible enough to handle *all problem types within a single model*. Since Labassi et al. (2022) needs to re-train for each instance type and only works for linear problems, we cannot test it against MIPLIB and MINLPLIB. Instead, we reproduce all benchmarks

⁵We are not aware of a learned BnB node-selection heuristic used for MINLPs, so guidance towards feature selection doesn’t exist yet. Taking advantage of them presumably also requires to train on nonlinear problems.

Table 2: Comparison against (Labassi et al., 2022). Note that we use a *single* network, evaluated out-of-distribution, while (Labassi et al., 2022) uses *different* networks, all trained on that specific type of mixed integer linear program. For all metrics, lower is better.

	FMCNF		GISP		WPMS	
	Nodes	Runtime	Nodes	Runtime	Nodes	Runtime
Labassi FMCNF	339.53 ± 5.90	29.45 ± 2.13	—	—	—	—
Labassi GISP	—	—	1219 ± 1.73	26.50 ± 1.55	—	—
Labassi WPMS	—	—	—	—	215.26 ± 1.97	10.46 ± 1.56
Ours	187.33 ± 3.67	19.99 ± 2.25	1216.16 ± 1.91	16.94 ± 1.49	221.73 ± 1.78	8.04 ± 1.72

used by Labassi et al. (2022) (each with their own separate models), and compare against them against our single model.

Labassi et al. (2022) considers the problem of *minimizing time-to-solution and minimizing the number of nodes explored* over a set of synthetic problems. This means that rather than the problem of minimizing the gap that can be reached within a given time limit (Table 1), here we always optimize to completion and track the runtime elapsed until the problem is solved. We use the “transfer” instances and best performing models provided by Labassi et al. (2022) and re-run the benchmarks on our hardware.

As we report in Table 2, we convincingly beat the prior work on every single benchmark (aside of WPMS node count), despite our method never having seen any of these problem types during training. This is surprising because Labassi et al. (2022) should have a convincing advantage due to the fact they not only have a dedicated agents for every single one of their problems, they also use the same generator for their training and testing instances. This implies that your single solver, evaluated out-of-distribution, manages to outperform the specialized agents proposed by Labassi et al. (2022) evaluated in-distribution. In general, our method improves upon Labassi et al. (2022) by between 30% and 56% with respect to runtime.

5.5 Ablations

We ablate the importance of the individual features used in our node selector using the SHAP (Lundberg & Lee, 2017) interpretability algorithm (see Appendix H). We find that our node selector automatically discovers best-practices from the classical node selection community, such as preferentially selecting nodes with lower lower-bound, balanced by greedy “best node” selection. Specifically interesting, we find that our selector significantly incorporates the amount of cutting planes applied to each node, hinting at a stronger than expected connection between node-utility and cutting planes.

In addition to the feature importance analysis done above, we also investigate running the model without a GNN: We find that when removing the GNN, the model tends to become very noisy and produce unreproducible experiments. Considering only the cases where the GNN-free model does well, we still find the model needs roughly 30% more nodes than the SCIP or our model with a GNN. More importantly, we notice the GNN-free model diverges during training: starting with a reward of roughly zero, the model diverges down to a reward of ≈ -0.2 , which amounts to a score roughly 20% worse than SCIP. We therefore conclude that, at least for our architecture, the GNN is necessary for both robustness and performance.

6 Limitations

There are still many open questions that give rise to future research or further investigation. First, while we report initial results in our ablation study (see Sec. 5.5 and Appendix H) on the importance of features, feature selection remains an area where we expect significant improvements, especially for nonlinear programming, which contemporary methods do not account for.

Second, one possible limitation is the limited runtime during training. Unfortunately, it is not computationally tractable for us to train on such large time-frames. However, we demonstrate in Sec. 5, that our model

trained on a 45s time limit generalizes flawlessly to larger time limits of 5min. Hence we also expect our method to work on considerably larger problem sets.

Third, we also expect significant improvements in performance through code optimization. An important area for research lies in generalized instance generation: Instead of focusing on single domain instances for training (e.g. from TSP), an instance generator should create problem instances with consistent, but varying levels of difficulty across different problem domains. Further, the number of nodes used before switching to classical node selectors is only done heuristically. Finding optimal switching points between different node selectors is still an open problem even beyond learned solutions and represents an interesting place for further research.

7 Conclusion

We have proposed a novel approach to branch-and-bound node selection, that uses the structure of the branch-and-bound process and reinforcement learning to convincingly beat classical SCIP and learnt node selectors. By aligning our model with the branch-and-bound tree structure, we have demonstrated the potential to develop a versatile heuristic that can be applied across various optimization problem domains, despite being trained on a narrow set of instances. To our knowledge, this is the first demonstration of learned node selection to mixed-integer (nonlinear) programming.

References

- Marcin Andrychowicz, Anton Raichuk, Piotr Stańczyk, Manu Orsini, Sertan Girgin, Raphael Marinier, Léonard Hussenot, Matthieu Geist, Olivier Pietquin, Marcin Michalski, Sylvain Gelly, and Olivier Bachem. What Matters In On-Policy Reinforcement Learning? A Large-Scale Empirical Study, June 2020.
- Jimmy Lei Ba, Jamie Ryan Kiros, and Geoffrey E Hinton. Layer normalization. *arXiv preprint arXiv:1607.06450*, 2016.
- Thomas C. Bachlechner, Bodhisattwa Prasad Majumder, Huanru Henry Mao, G. Cottrell, and Julian McAuley. Rezero is all you need: Fast convergence at large depth. In *Conference on Uncertainty in Artificial Intelligence*, 2020. URL <https://api.semanticscholar.org/CorpusID:212644626>.
- Christopher Bayliss, Geert De Maere, Jason Adam David Atkin, and Marc Paelinck. A simulation scenario based mixed integer programming approach to airline reserve crew scheduling under uncertainty. *Annals of Operations Research*, 252:335–363, 2017.
- Ksenia Bestuzheva, Mathieu Besançon, Wei-Kun Chen, Antonia Chmiela, Tim Donkiewicz, Jasper van Doornmalen, Leon Eifler, Oliver Gaul, Gerald Gamrath, Ambros Gleixner, Leona Gottwald, Christoph Graczyk, Katrin Halbig, Alexander Hoen, Christopher Hojny, Rolf van der Hulst, Thorsten Koch, Marco Lübbecke, Stephen J. Maher, Frederic Matter, Erik Mühmer, Benjamin Müller, Marc E. Pfetsch, Daniel Rehfeldt, Steffan Schlein, Franziska Schlösser, Felipe Serrano, Yuji Shinano, Boro Sofranac, Mark Turner, Stefan Vigerske, Fabian Wegscheider, Philipp Wellner, Dieter Weninger, and Jakob Witzig. The SCIP Optimization Suite 8.0. Technical report, Optimization Online, December 2021.
- Ksenia Bestuzheva, Antonia Chmiela, Benjamin Müller, Felipe Serrano, Stefan Vigerske, and Fabian Wegscheider. Global Optimization of Mixed-Integer Nonlinear Programs with SCIP 8, January 2023.
- Jakob Bossek, Pascal Kerschke, Aneta Neumann, Markus Wagner, Frank Neumann, and Heike Trautmann. Evolving diverse tsp instances by means of novel and creative mutation operators. In *Proceedings of the 15th ACM/SIGEVO Conference on Foundations of Genetic Algorithms*, FOGA '19, pp. 58–71, New York, NY, USA, 2019. Association for Computing Machinery. ISBN 9781450362542. doi: 10.1145/3299904.3340307.
- Michael R. Bussieck, Arne Stolbjerg Drud, and Alexander Meeraus. MINLPLib—a collection of test models for mixed-integer nonlinear programming. *INFORMS Journal on Computing*, 15(1):114–119, February 2003. doi: 10.1287/ijoc.15.1.114.15159.
- William J Cook, David L Applegate, Robert E Bixby, and Vasek Chvatal. *The traveling salesman problem: a computational study*. Princeton university press, 2011.

- George B. Dantzig. Reminiscences about the origins of linear programming. *Operations Research Letters*, 1(2):43–48, 1982. ISSN 0167-6377. doi: [https://doi.org/10.1016/0167-6377\(82\)90043-8](https://doi.org/10.1016/0167-6377(82)90043-8).
- Aveen Dayal, Linga Reddy Cenkeramaddi, and Ajit Jha. Reward criteria impact on the performance of reinforcement learning agent for autonomous navigation. *Applied Soft Computing*, 126:109241, 2022. ISSN 1568-4946. doi: <https://doi.org/10.1016/j.asoc.2022.109241>. URL <https://www.sciencedirect.com/science/article/pii/S1568494622004586>.
- Marc Etheve, Zacharie Alès, Côme Bissuel, Olivier Juan, and Safia Kedad-Sidhoum. Reinforcement learning for variable selection in a branch and bound algorithm. *ArXiv*, abs/2005.10026, 2020. URL <https://api.semanticscholar.org/CorpusID:211551730>.
- Christodoulos A. Floudas and Xiaoxia Lin. Mixed integer linear programming in process scheduling: Modeling, algorithms, and applications. *Annals of Operations Research*, 139:131–162, 2005.
- Maxime Gasse, Didier Chételat, Nicola Ferroni, Laurent Charlin, and Andrea Lodi. Exact combinatorial optimization with graph convolutional neural networks. In *Neural Information Processing Systems*, 2019. URL <https://api.semanticscholar.org/CorpusID:174797862>.
- Maxime Gasse, Quentin Cappart, Jonas Charfreitag, Laurent Charlin, Didier Chételat, Antonia Chmiela, Justin Dumouchelle, Ambros M. Gleixner, Aleksandr M. Kazachkov, Elias Boutros Khalil, Pawel Lichocki, Andrea Lodi, Miles Lubin, Chris J. Maddison, Christopher Morris, Dimitri J. Papageorgiou, Augustin Parjadis, Sebastian Pokutta, Antoine Prouvost, Lara Scavuzzo, Giulia Zarpellon, Linxin Yangm, Sha Lai, Akang Wang, Xiaodong Luo, Xiang Zhou, Haohan Huang, Sheng Cheng Shao, Yuanming Zhu, Dong Zhang, Tao Manh Quan, Zixuan Cao, Yang Xu, Zhewei Huang, Shuchang Zhou, Cheng Binbin, He Minggui, Hao Hao, Zhang Zhiyu, An Zhiwu, and Mao Kun. The machine learning for combinatorial optimization competition (ml4co): Results and insights. *ArXiv*, abs/2203.02433, 2022. URL <https://api.semanticscholar.org/CorpusID:247245014>.
- Alan E. Gelfand and Adrian F. M. Smith. Sampling-based approaches to calculating marginal densities. *Journal of the American Statistical Association*, 85(410):398–409, 1990. ISSN 01621459. URL <http://www.jstor.org/stable/2289776>.
- Ambros Gleixner, Gregor Hendel, Gerald Gamrath, Tobias Achterberg, Michael Bastubbe, Timo Berthold, Philipp Christophel, Kati Jarck, Thorsten Koch, Jeff Linderoth, Marco Lübbecke, Hans D. Mittelmann, Derya Ozyurt, Ted K. Ralphs, Domenico Salvagnin, and Yuji Shinano. MIPLIB 2017: Data-driven compilation of the 6th mixed-integer programming library. *Mathematical Programming Computation*, 13(3):443–490, September 2021. ISSN 1867-2957. doi: 10.1007/s12532-020-00194-3.
- He He, Hal Daume III, and Jason M Eisner. Learning to search in branch and bound algorithms. In Z. Ghahramani, M. Welling, C. Cortes, N. Lawrence, and K.Q. Weinberger (eds.), *Advances in Neural Information Processing Systems*, volume 27. Curran Associates, Inc., 2014.
- Shengyi Huang, Rousslan Fernand Julien Dossa, Chang Ye, and Jeff Braga. Cleanrl: High-quality single-file implementations of deep reinforcement learning algorithms. *ArXiv*, abs/2111.08819, 2021. URL <https://api.semanticscholar.org/CorpusID:260421728>.
- Shengyi Huang, Rousslan Fernand Julien Dossa, Antonin Raffin, Anssi Kanervisto, and Weixun Wang. The 37 implementation details of proximal policy optimization. In *ICLR Blog Track*, 2022. URL <https://iclr-blog-track.github.io/2022/03/25/ppo-implementation-details/>. <https://iclr-blog-track.github.io/2022/03/25/ppo-implementation-details/>.
- Diederik P. Kingma and Max Welling. Auto-encoding variational bayes. *CoRR*, abs/1312.6114, 2013. URL <https://api.semanticscholar.org/CorpusID:216078090>.
- Yuri Kochetov and Dmitry Ivanenko. *Computationally Difficult Instances for the Uncapacitated Facility Location Problem*, pp. 351–367. Springer US, Boston, MA, 2005. ISBN 978-0-387-25383-1. doi: 10.1007/0-387-25383-1_16.

- Abdel Ghani Labassi, Didier Chételat, and Andrea Lodi. Learning to compare nodes in branch and bound with graph neural networks. In *Advances in Neural Information Processing Systems 35*, 2022.
- Ilya Loshchilov and Frank Hutter. Fixing weight decay regularization in adam. *ArXiv*, abs/1711.05101, 2017. URL <https://api.semanticscholar.org/CorpusID:3312944>.
- Scott M. Lundberg and Su-In Lee. A unified approach to interpreting model predictions. In *Neural Information Processing Systems*, 2017. URL <https://api.semanticscholar.org/CorpusID:21889700>.
- Govind Menon, M. Nabil, and Sridharakumar Narasimhan. Branch and bound algorithm for optimal sensor network design. *IFAC Proceedings Volumes*, 46(32):690–695, 2013. ISSN 1474-6670. doi: <https://doi.org/10.3182/20131218-3-IN-2045.00143>. 10th IFAC International Symposium on Dynamics and Control of Process Systems.
- C. E. Miller, A. W. Tucker, and R. A. Zemlin. Integer programming formulation of traveling salesman problems. *J. ACM*, 7(4):326–329, oct 1960. ISSN 0004-5411. doi: 10.1145/321043.321046.
- Hans D. Mittelmann. Decison Tree for Optimization Software. <https://plato.asu.edu/sub/nlores.html>, 2021. Accessed: 2023-09-02.
- Volodymyr Mnih, Koray Kavukcuoglu, David Silver, Alex Graves, Ioannis Antonoglou, Daan Wierstra, and Martin A. Riedmiller. Playing atari with deep reinforcement learning. *ArXiv*, abs/1312.5602, 2013. URL <https://api.semanticscholar.org/CorpusID:15238391>.
- Volodymyr Mnih, Koray Kavukcuoglu, David Silver, Andrei A. Rusu, Joel Veness, Marc G. Bellemare, Alex Graves, Martin Riedmiller, Andreas K. Fidjeland, Georg Ostrovski, Stig Petersen, Charles Beattie, Amir Sadik, Ioannis Antonoglou, Helen King, Dhharshan Kumaran, Daan Wierstra, Shane Legg, and Demis Hassabis. Human-level control through deep reinforcement learning. *Nature*, 518(7540):529–533, February 2015. doi: 10.1038/nature14236. URL <https://doi.org/10.1038/nature14236>.
- Volodymyr Mnih, Adrià Puigdomènech Badia, Mehdi Mirza, Alex Graves, Timothy P. Lillicrap, Tim Harley, David Silver, and Koray Kavukcuoglu. Asynchronous methods for deep reinforcement learning. In *International Conference on Machine Learning*, 2016. URL <https://api.semanticscholar.org/CorpusID:6875312>.
- David R. Morrison, Sheldon H. Jacobson, Jason J. Sauppe, and Edward C. Sewell. Branch-and-bound algorithms: A survey of recent advances in searching, branching, and pruning. *Discrete Optimization*, 19: 79–102, 2016. ISSN 1572-5286. doi: <https://doi.org/10.1016/j.disopt.2016.01.005>.
- Lars Otten and Rina Dechter. A Case Study in Complexity Estimation: Towards Parallel Branch-and-Bound over Graphical Models. *Uncertainty in Artificial Intelligence - Proceedings of the 28th Conference, UAI 2012*, October 2012.
- Christopher W. F. Parsonson, Alexandre Laterre, and Thomas D. Barrett. Reinforcement learning for branch-and-bound optimisation using retrospective trajectories. In *AAAI Conference on Artificial Intelligence*, 2022. URL <https://api.semanticscholar.org/CorpusID:249192146>.
- Max B. Paulus, Giulia Zarpellon, Andreas Krause, Laurent Charlin, and Chris J. Maddison. Learning to cut by looking ahead: Cutting plane selection via imitation learning. In *International Conference on Machine Learning*, 2022. URL <https://api.semanticscholar.org/CorpusID:250072284>.
- Ronald L. Rardin, Craig A. Tovey, and Martha G. Pilcher. Analysis of a Random Cut Test Instance Generator for the TSP. In *Complexity in Numerical Optimization*, pp. 387–405. WORLD SCIENTIFIC, July 1993. ISBN 978-981-02-1415-9. doi: 10.1142/9789814354363_0017.
- Gerhard Reinelt. TSPLIB—a traveling salesman problem library. *ORSA Journal on Computing*, 3(4):376–384, November 1991. doi: 10.1287/ijoc.3.4.376.
- Christian P. Robert and Gareth O. Roberts. Rao-blackwellization in the mcmc era. 2021. URL <https://api.semanticscholar.org/CorpusID:230437867>.

- Lara Scavuzzo, F. Chen, Didier Ch'etelat, Maxime Gasse, Andrea Lodi, N. Yorke-Smith, and Karen I. Aardal. Learning to branch with tree mdps. *ArXiv*, abs/2205.11107, 2022. URL <https://api.semanticscholar.org/CorpusID:248987388>.
- J. Schulman, Philipp Moritz, S. Levine, Michael I. Jordan, and P. Abbeel. High-Dimensional Continuous Control Using Generalized Advantage Estimation. *CoRR*, June 2015.
- John Schulman, Filip Wolski, Prafulla Dhariwal, Alec Radford, and Oleg Klimov. Proximal policy optimization algorithms. *ArXiv*, abs/1707.06347, 2017.
- David Silver, Thomas Hubert, Julian Schrittwieser, Ioannis Antonoglou, Matthew Lai, Arthur Guez, Marc Lanctot, L. Sifre, Dharshan Kumaran, Thore Graepel, Timothy P. Lillicrap, Karen Simonyan, and Demis Hassabis. Mastering chess and shogi by self-play with a general reinforcement learning algorithm. *ArXiv*, abs/1712.01815, 2017. URL <https://api.semanticscholar.org/CorpusID:33081038>.
- Richard S Sutton and Andrew G Barto. *Reinforcement learning: An introduction*. MIT press, 2018.
- Yunhao Tang, Shipra Agrawal, and Yuri Faenza. Reinforcement learning for integer programming: Learning to cut. *ArXiv*, abs/1906.04859, 2019. URL <https://api.semanticscholar.org/CorpusID:186206599>.
- Mark Turner, Thorsten Koch, Felipe Serrano, and Michael Winkler. Adaptive cut selection in mixed-integer linear programming. *Open J. Math. Optim.*, 4:1–28, 2022. URL <https://api.semanticscholar.org/CorpusID:247026030>.
- Eleonora Vercesi, Stefano Gualandi, Monaldo Mastrolilli, and Luca Maria Gambardella. On the generation of metric TSP instances with a large integrality gap by branch-and-cut. *Mathematical Programming Computation*, 15(2):389–416, June 2023. ISSN 1867-2957. doi: 10.1007/s12532-023-00235-7.
- Zhihai Wang, Xijun Li, Jie Wang, Yufei Kuang, Min jie Yuan, Jianguo Zeng, Yongdong Zhang, and Feng Wu. Learning cut selection for mixed-integer linear programming via hierarchical sequence model. *ArXiv*, abs/2302.00244, 2023. URL <https://api.semanticscholar.org/CorpusID:256459559>.
- Bing Xu, Naiyan Wang, Tianqi Chen, and Mu Li. Empirical evaluation of rectified activations in convolutional network. *ArXiv*, abs/1505.00853, 2015. URL <https://api.semanticscholar.org/CorpusID:14083350>.
- Kaan Yilmaz and Neil Yorke-Smith. A Study of Learning Search Approximation in Mixed Integer Branch and Bound: Node Selection in SCIP. *AI*, 2(2):150–178, April 2021. ISSN 2673-2688. doi: 10.3390/ai2020010.

Appendix

A Features

Table 3 lists the features used on every individual node. The features split into two different types: One being “model” features, the other being “node” features. Model features describe the state of the entire model at the currently explored node, while node features are specific to the yet-to-be-solved added node. We aim to normalize all features with respect to problem size, as e. g., just giving the lower-bound to a problem is prone to numerical domain shifts. For instance a problem with objective $c^T x, x \in P$ is inherently the same from a solver point-of-view as a problem $10c^T x, x \in P$, but would give different lower-bounds. Since NNs are generally nonlinear estimators, we need to make sure such changes do not induce huge distribution shifts. We also clamp the feature values between $[-10, 10]$ which represent “infinite” values, which can occur, for example in the optimality gap. Last but not least, we standardize features using empirical mean and standard deviation. These features are inspired by prior work, such as Labassi et al. (2022); Yilmaz & Yorke-Smith

Table 3: Features used per individual node.

model features	Number of cuts applied	normalized by total number of constraints
	Number of separation rounds	
	optimality gap	
	lp iterations	
	mean integrality gap	
	percentage of variables already integral	
	histogram of fractional part of variables	10 evenly sized buckets
node features	depth of node	normalized by total number of nodes
	node lowerbound	normalized by min of primal and dual bound
	node estimate	normalized by min of primal and dual bound

(2021), but adapted to the fact that we do not need e. g., explicit entries for the left or right child’s optimality gap, as these (and more general K-step versions of these) can be handled by the GNN.

Further, to make batching tractable, we aim to have constant size features. This is different from e. g., Labassi et al. (2022), who utilize flexibly sized graphs to represent each node. The upside of this approach is that certain connections between variables and constraints may become more apparent, with the downside being the increased complexity of batching these structures and large amounts of nodes used. This isn’t a problem for them, as they only consider pairwise comparisons between nodes, rather than the entire branch-and-bound graph, but for us would induce a great deal of complexity and computational overhead, especially in the larger instances. For this reason, we represent flexibly sized inputs, such as the values of variables, as histograms: i.e., instead of having k nodes for k variables and wiring them together, we produce once distribution of variable values with 10-buckets, and feed this into the network. This loses a bit of detail in the representation, but allows us to scale to much larger instances than ordinarily possible.

In general, these features are not optimized, and we would expect significant improvements from more well-tuned features. Extracting generally meaningful features from branch-and-bound is a nontrivial task and is left as a task for future work.

B Theoretical Derivation

One naive way of parameterizing actions is selecting probabilistically by training the probability of going to the left or right child at any node. This effectively gives a hierarchical Bernoulli description of finding a path in the tree. A path is simply a sequence of left (“zero direction”) and right (“one direction”) choices, with the total probability of observing a path being the likelihood of observing a specific chain

$$p(\text{leaf}) = \prod_{i \in \mathcal{P}(\text{root}, \text{leaf})} p_i,$$

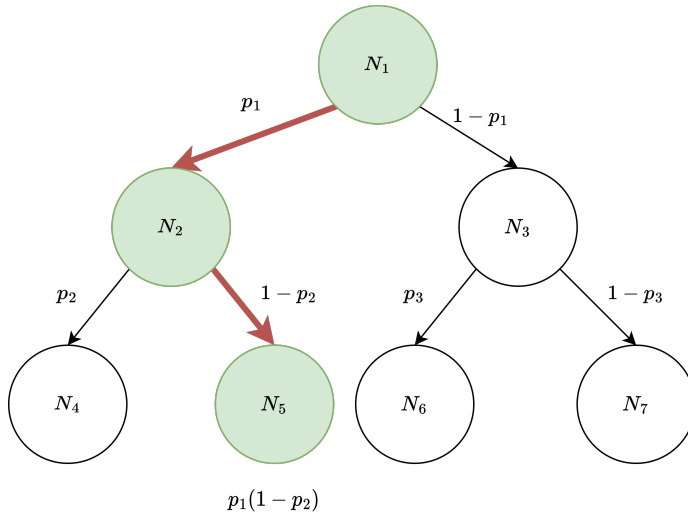


Figure 2: Naive approach using recursive selection. The probabilities are computed based on which “fork” of the tree is traveled. Sampling this can be done by sampling left or right based on p_i

with p_i being the i ’th decision in the graph (see Fig 2). Node selection can now be phrased as the likelihood of a random (weighted) walk landing at the specified node. However, using this parametrization directly would yield a significant number of problems:

Removing illegal paths from the model is quite challenging to do with sufficiently high performance. If a node gets pruned or fully solved, the probability to select this node has to be set to zero. This information has to be propagated upward the tree to make sure that the selection never reaches a “dead-end”. This is possible, but turns out to be rather expensive to compute since it needs to evaluate the entire tree from leaves to root.

From a theoretical point of view, the hierarchical Bernoulli representation also has a strong prior towards making selections close to the root, as the probability of reaching a node a depth K consists of $p_1 \cdot p_2 \cdots p_K$ selections. Since all p_i are set to an uninformative prior $0 < p_i < 1$, the model at initialization has an increased likelihood to select higher nodes in the tree. Considering that classical methods specifically mix plunging heuristics into their selection to get increased depth exploration (see Sec. 3), this “breadth over depth” initialization is expected to give low performance. Therefore, one would need to find a proper initialization that allows the model to e.g., uniformly select nodes independent of depth to get good initialization.

The fact that multiple sampling sites exist in this method also poses issues with RL, as small errors early in the tree can have catastrophic effects later. This means the tree based model is a significantly higher variance estimator than the estimator we propose in Sec 4.3, which yields much worse optimization characteristics. It is well established in existing deep learning (e.g., (Kingma & Welling, 2013)) and general Bayesian Inference (e.g., (Robert & Roberts, 2021; Gelfand & Smith, 1990)) literature, that isolating or removing sampling sites can lead to lower variance, and therefore much more performant, statistical estimators.

Using those insights, we can now rewrite this naive approach into the one we propose in Sec. 4.3: First, instead of sampling just one path, we can sample *all* possible paths and compute the likelihood for each. The result will be a probability p at every possible leaf. If one parameterizes this as a logarithmic probability **the likelihood of sampling any individual leaf**, can be written as

$$\log p_{\text{leaf}} = \sum_{i \in P(\text{root}, \text{leaf})} \log p_i. \quad (13)$$

We can further assume that the $\log p$ ’s are given as *unnormalized logits* W' and only normalize them at the end such that to likelihood of all leaves together is 1.

This already gives an increase in performance, as the paths can be computed in parallel *without* needing iterated random sampling, which tends to be a very expensive operation. One also has fewer discrete choices,

meaning fewer backpropagation graph-breaks, which improves overall stability. The change to unnormalized logits acts essentially as a reparametrization trick (for other examples of reparametrization, see (Kingma & Welling, 2013)).

If one considers unnormalized log-probabilities, which have a range $(-\infty, \infty)$, this scheme becomes very similar to the one we ended up using in Sec. 4.3. Let $f(\text{node}, \text{tree})$ denote the unnormalized probabilities such that $p(\text{node}, \text{tree}) = \frac{f(\text{node}, \text{tree})}{Z}$. One can compute the likelihood of selecting a specific node as:

$$\begin{aligned}
 p(\text{leaf}|\text{tree}) &= \frac{f(\text{leaf}, \text{tree})}{\sum_{c \in \mathcal{C}} f(c, \text{tree})} && \text{normalization} \\
 &= \frac{\exp(\log(f(\text{leaf}, \text{tree})))}{\sum_{c \in \mathcal{C}} \exp(\log(f(c, \text{tree})))} && \log f \text{ are unnormalized logits} \\
 &= \frac{\exp(W'(\text{leaf}))}{\sum_{c \in \mathcal{C}} \exp(W'(c))} && \text{definition } W' \text{ as unnormalized logit} \\
 &= \text{softmax}_{\text{leaf}}\{W'(c) | \forall c \in \mathcal{C}\} && \text{definition softmax,}
 \end{aligned}$$

where $\text{softmax}_{\text{leaf}}$ refers to the softmax-entry associated with leaf. The resulting decomposition is, while not the same, equivalent to the original Bernoulli decomposition (in the sense that for any Bernoulli decomposition there exists a softmax-based decomposition). Beyond the massive reduction in sampling sites from $O(\text{depth})$ to a single sampling site, phrasing the problem using unnormalized-log p representations gives rise to additional optimizations:

Firstly, to achieve uniform likelihood for all nodes at the beginning of training, we simply have to initialize $W(n) = 0$ for all nodes, which can be done by setting the output weights and biases to zero (in practice we set bias to zero and weights to a small random value).

Secondly to account for pruned or solved nodes, we do not need to change the unnormalized probabilities. Instead, we simply only sample the paths associated with selectable nodes, as we know the likelihood of selecting a pruned or solved node is zero. This means we can restrict ourselves to only evaluating the candidate paths \mathcal{C} , rather than all paths (see Eq. 9).

The last modification we made in our likelihood computation (see Eq. 8), is to normalize the weights based on depth. This is done mainly for numerical stability, but in our Bayesian framework is equivalent to computing the softmax-normalization Eq. 9 using weights inversely proportional to depth. The resulting algorithm is much more stable and performant than the naive parametrization. In early implementations we used the recursive-sampling approach to compute likelihoods, but the resulting scheme did not manage to reach above random results on the training set, presumably due to the higher computational burden and worse initialization. There are also other advantages to our parametrization, such as the fact that one can easily include a sampling temperature τ into the process

$$\text{node} \sim \text{softmax}\{W'(c)/\tau | \forall c \in \mathcal{C}\}$$

which can be nice to tune the model more into the direction ‘‘exploitation’’ during testing. For our later benchmarking (Sec 5) we keep $\tau = 1$ (i.e., no temperature), as it would introduce a further tunable hyperparameter, but this could be interesting for future work.

This construction has interesting parallels to Monte-Carlo Tree Search (MCTS) Silver et al. (2017) based reinforcement learning methods. The difference in our method is that we consider iterative updates to a policy distribution π rather than a Q-function, and therefore can be seen as a policy-based tree search scheme: While traditional MCTS uses variants of UCB-scores to guide the search, our method can be thought of as variants of Thompson sampling to facilitate the exploration-exploitation tradeoff. We leave a more thorough investigation of this to future work.

Table 4: Performance across benchmarks (the policy only saw TSP instances during training). The 5min runs use the same model, evaluated for the first 650 nodes, and processed according to Sec. 5.1.

Benchmark	Reward	Utility	Utility/Node	Win-rate	geo-mean Ours	geo-mean SCIP
TSPLIB (Reinelt, 1991)	0.184	0.030	0.193	0.50	0.931	0.957
UFLP (Kochetov & Ivanenko, 2005)	0.078	0.093	-0.064	0.636	0.491	0.520
MINLPLib (Bussieck et al., 2003)	0.487	0.000	0.114	0.852	28.783	31.185
MIPLIB (Gleixner et al., 2021)	0.140	-0.013	0.208	0.769	545.879	848.628
TSPLIB@5min	0.192	0.056	0.336	0.600	1.615	2.000
MINLPLib@5min	0.486	-0.012	0.078	0.840	17.409	20.460
MIPLib@5min	0.150	-0.075	0.113	0.671	66.861	106.400

C Additional metrics

Aside from the previously discussed Reward in Section 4.1, we also considered two different ways of measuring the quality of our method compared to SCIP. While both of these have theoretical problems, we still find them interesting to consider as they act as additional reference points for the behavior of the policies.

Utility defines the *difference* between both methods normalized using the maximum of both gaps:

$$\text{Utility} = \left(\frac{\text{gap}(\text{scip}) - \text{gap}(\text{node selector})}{\max(\text{gap}(\text{node selector}), \text{gap}(\text{scip}))} \right). \quad (14)$$

The reason we do not use this as a reward measure is because we empirically found it to produce worse models. This is presumably because some of the negative attributes of our reward, e.g., the asymmetry of the reward signal, lead to more robust policies. In addition, the utility metric gives erroneous measurements when both models hit zero optimality gap. This is because utility implicitly defines $\frac{0}{0} = 0$, rather than reward, which defines it as $\frac{0}{0} = 1$. In some sense the utility measurement is accurate, in that our method does not improve upon the baseline. On the other hand, our method is already provably optimal as soon as it reaches a gap of 0%. In general, utility compresses the differences more than reward which may or may not be beneficial in practice.

Utility per Node normalizes Utility by the number of nodes used during exploration:

$$\text{Utility/Node} = \left(\frac{\text{scip} - \text{selector}}{\max(\text{selector}, \text{scip})} \right), \quad (15a)$$

where $\text{selector} = \frac{\text{gap}(\text{node selector})}{\text{nodes}(\text{node selector})}$ and $\text{scip} = \frac{\text{gap}(\text{scip})}{\text{nodes}(\text{scip})}$. The per-node utility gives a proxy for the total amount of “work” done by each method. However, it ignores the individual node costs, as solving the different LPs may take different amounts of resources (a model with higher “utility/node” is not necessarily more efficient as our learner might pick cheap but lower expected utility nodes on purpose). Further, the metric is underdefined: comparing two ratios, a method may become better by increasing the number of nodes processed, but keeping the achieved gap constant. In practice the number of nodes processed by our node selector is dominated by the implementation rather than the node choices, meaning we can assume it is invariant to changes in policy. Another downside arises if both methods reach zero optimality gap, the resulting efficiency will also be zero regardless of how many nodes we processed. As our method tend to reach optimality much faster (see Sec. 5 and Appendix I), all utility/node results can be seen as a lower-bound for the actual efficiency.

D Comparisons of Runtime to completion

We also compare the runtime of our selector against the SCIP baseline on TSPLIB. For this we set a maximum time limit of 30min and run both methods. It is worth noting that due to the inherent difficulty of TSPLIB, a significant number of problems are still unsolved after 30min, in which case these models are simply assigned the maximum time as their overall completion time. Note that this also implies that the SCIP solver itself not capable of solving these problems due to their scale. We reckon that this is also the reason why e.g., Labassi

Method	Runtime shifted geometric mean	Nodes Processed geometric mean
SCIP	1016.61s	4122.67
Ours	1003.03s	2735.33

Table 5: The shifted geometric mean (shifted by +10) of runtime and number of nodes processed.

et al. (2022) does not even attempt to benchmark on these large scale problems. Our method outperforms the baseline, however due to the fact that our method aims to improve the quality of early selections in particular, the amount of improvement is rather small. Further, our method is fundamentally undertrained to adequately deal with longer time horizons and we would assume the effect of our method is larger the longer the model is trained. Despite this being a worst-case evaluation scenario, our method manages to outperform the baseline in both runtime and number of nodes needed.

Interestingly, we also manage to reach this superior performance while utilizing only about half the number of nodes. This discrepancy cannot be explained by just considering the slowdown due to our policy needing to be evaluated, as, while it is a significant overhead due to the Python implementation, it is very far from being large enough to justify a 50% slowdown over the course of 30min. This also shows more generally that even if one restricts themselves to only processing the beginning of the branch-and-bound tree, one can reach superior performance to the standard node-selection schemes.

E Architecture

Our network consists of two subsystems: First, we have the feature embedder that transforms the raw features into embeddings, without considering other nodes this network consists of one linear layer $|d_{features}| \rightarrow |d_{model}|$ with LeakyReLU (Xu et al., 2015) activation followed by two $|d_{model}| \rightarrow |d_{model}|$ linear layers (activated by LeakyReLU) with skip connections. We finally normalize the outputs using a LayerNorm (Ba et al., 2016) *without* trainable parameters (i. e., just shifting and scaling the feature dimension to a normal distribution).

Second, we consider the GNN model, whose objective is the aggregation across nodes according to the tree topology. This consists of a single LeakyReLU activated layer with skip-connections. We use ReZero (Bachlechner et al., 2020) initialization to improve the convergence properties of the network. Both the weight and value heads are simple linear projections from the embedding space. Following the guidance in (Andrychowicz et al., 2020), we make sure the value and weight networks are independent by detaching the value head’s gradient from the embedding network.

For this work we choose $|d_{model}| = 512$, but we did not find significant differences between different model sizes past a width of 256. For training we use AdamW Loshchilov & Hutter (2017) with a standard learning rate of $3 \cdot 10^{-4}$ and default PPO parameters.

F TSP-as-MILP Formulation

In general, due to the fact that TSP is amongst the most studied problems in discrete optimization, we can expect existing mixed-integer programming systems to have rich heuristics that provide a strong baseline for

our method. Mathematically, we choose the Miller–Tucker–Zemlin (MTZ) formulation (Miller et al., 1960):

$$\begin{aligned}
\min_x \quad & \sum_{i=1}^n \sum_{j \neq i, j=1}^n c_{ij} x_{ij} \\
\text{subject to} \quad & \sum_{j=1, i \neq j}^n x_{ij} = 1 && \forall i = 1, \dots, n \\
& \sum_{i=1, i \neq j}^n x_{ij} = 1 && \forall j = 1, \dots, n \\
& u_1 - u_j + (n-1)x_{ij} \leq n-2 && 2 \leq i \neq j \leq n \\
& 2 \leq u_i \leq n && 2 \leq i \leq n \\
& u_i \in \mathbb{Z}, x_{ij} \in \{0, 1\}
\end{aligned}$$

Effectively this formulation keeps two buffers: one being the actual (i, j) -edges travelled x_{ij} , the other being a node-order variable u_i that makes sure that $u_i < u_j$ if i is visited before j . There are alternative formulations, such as the Dantzig–Fulkerson–Johnson (DFJ) formulation, which are used in modern purpose-built TSP solvers, but those are less useful for general problem generation: The MTZ formulation essentially relaxes the edge-assignments and order constraints, which then are branch-and-bounded into hard assignments during the solving process. This is different to DFJ, which instead relaxes the “has to pass through all nodes” constraint. DFJ allows for subtours (e.g., only contain node A, B, C but not D, E) which then get slowly eliminated via the on-the-fly generation of additional constraints. To generate these constraints one needs specialised row-generators which, while very powerful from an optimization point-of-view, make the algorithm less general as a custom row-generator has to intervene into every single node. However, in our usecase we also do not really care about the ultimate performance of individual algorithms as the reinforcement learner only looks for improvements to the existing node selections. This means that as long as the degree of improvement can be adequately judged, we do not need state-of-the-art solver implementations to give the learner a meaningful improvement signal.

G Uncapacitated facility location Problem

Mathematically, the uncapacitated facility location problem can be seen as sending a product z_{ij} from facility i to consumer j with cost c_{ij} and demand d_j . One can only send from i to j if facility i was built in the first place, which incurs cost f_i . The overall problem therefore is

$$\begin{aligned}
\min_x \quad & \sum_{i=1}^n \sum_{j=1}^m c_{ij} d_j z_{ij} + \sum_{i=0}^n f_i x_i \\
\text{subject to} \quad & \sum_{j=1, i \neq j}^n z_{ij} = 1 && \forall i = 1, \dots, m \\
& \sum_{i=1, i \neq j}^n z_{ij} \leq M x_i && \forall j = 1, \dots, n \\
& z_{ij} \in \{0, 1\} && \forall i, j = 1, \dots, n \\
& x_i \in \{0, 1\} && \forall i = 1, \dots, n
\end{aligned}$$

where M is a suitably large constant representing the infinite-capacity one has when constructing $x_i = 1$. One can always choose $M \geq m$ since that, for the purposes of the polytop is equivalent to setting M to literal infinity. This is also sometimes referred to as the “big M ” method.

The instance generator by Kochetov & Ivanenko (2005) works by setting $n = m = 100$ and setting all opening costs at 3000. Every city has 10 “cheap” connections sampled from $\{0, 1, 2, 3, 4\}$ and the rest have cost 3000, which represents infinity (i.e., also invoking the big M method).

H Feature Importance

We try to interpret the learned node-selection heuristic by applying the KernelSHAP (Lundberg & Lee, 2017) method. SHAP methods try to estimate the feature importance by measuring the performance of an estimator where some portion of the features are replaced with a “neutral” element. Doing this with a large enough set, one is able to extract the feature importance in the form of the magnitude of the change between the expected value of the estimator and the value the estimator would have had if a specific feature were absent.

Analyzing our RL method with SHAP has two significant limitations: Firstly, we ignore the impact of message passing on the model and instead analyze every node as a leaf node. This is of relatively small impact as the time where a node was selected it had to have been a leaf node anyways, so the plots faithfully show the model output at selection time.

The second limitation is that we do not have an iid. dataset, but instead have to build one from the environment first. To build that dataset, we could sample random BnB trees and evaluate on the nodes, but this would mean we evaluate our model completely out-of-distribution, as random selection will most likely lead to states the model would never want to reach and is therefore ill equipped to handle. Therefore, we instead build our dataset by running our node-selector on a subset of MIPLIB to gather our importance-evaluation data. This has the downside that the expected value of our selection network is higher than in random selection, since the model is guided towards selecting higher value nodes.

With these caveats in mind, one can see in fig. 3 that our node selector relies significantly on the node lowerbound for setting its weight. This makes sense: in node-selection there is a fundamental tension between raising the lower bound and opportunistically searching for new primal solutions. The current SCIP default “hybrid best bound search” does exactly that, just using hand-made heuristics where a nodes are selected based on a mixture of following the currently best bound nodes, and plunging depth-first search to find better solutions. However, as can be seen in our benchmarks (tab 1), we beat SCIP’s default selector quite significantly, which implies a nontrivial interaction in the remaining features.

Looking at the beeswarm plot 4, we observe that our model preferentially picks nodes which, in addition to a low node lowerbound, also uses nodes which have few variables with an integrality gap of 0.2 and 0.3, has a lot of cuts applied, and has a high expected integrality gap. If we considered a node with all of these features (and assume there would not be any nonlinear value-dampening effects), such a node would be a prime candidate for having good child nodes: A node with a low lowerbound means that the node still has significant room for improvement, while having a lot of cuts applied means that the node’s solution is sufficiently close to existing integral points to make it feasible to find better values. Looking further into the features, one can also see that the model dislikes nodes that already have a significant number of “already integral” variables. This makes sense as nodes with a significant number of integral variables that are not solved already (i.e., they have children to split on), can be quite hard to complete while not giving a significant improvement in solution quality. This is because most likely a primal heuristic has already found the optimal value of that node, but branch-and-bound still needs a significant number of trials to prove that the found value is optimal in that subtree.

In short, our solver picks the nodes with the highest degree of possible improvement (low lowerbound), while also favoring nodes that have more information (more cuts applied) and presumably are nontrivial to solve via heuristics (high mean to integral gap/low “already integral” ratio).

In general, interpreting dynamic RL policies is highly nontrivial, especially if the estimator is nonlinear, but the interactions we can clearly see in the SHAP plots indicates that the learned policy is reasonably well grounded in existing best-practices for node selectors.

I Full Results

The following two sections contain the per-instance results on the two “named” benchmarks TSPLIB (Reinelt, 1991) and MINLPLIB (Bussieck et al., 2003). We test against the strong SCIP 8.0.4 baseline. Due to compatibility issues, we decided not to test against (Labassi et al., 2022) or (He et al., 2014): These

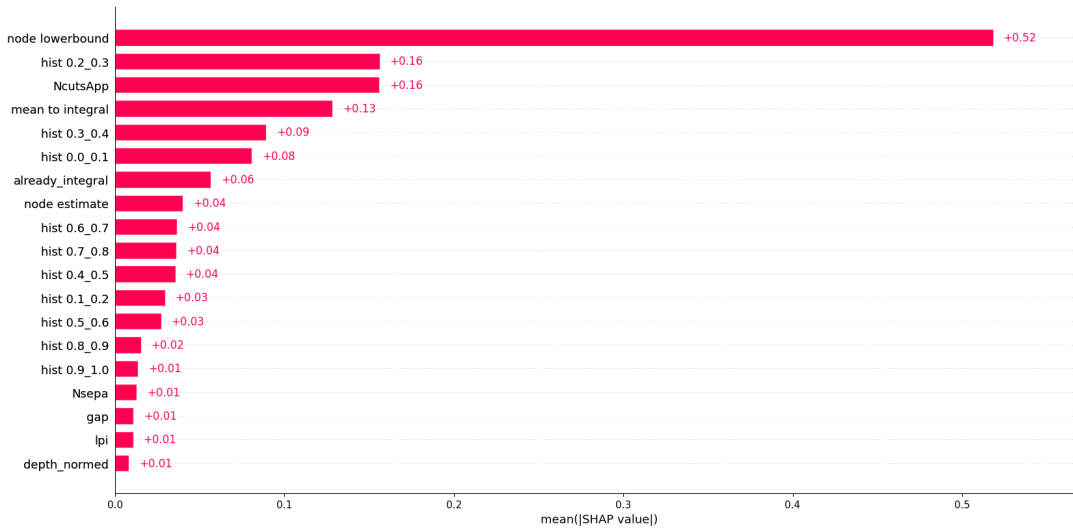


Figure 3: Barplot showing feature importance of individual nodes using the KernelSHAP (Lundberg & Lee, 2017) method.

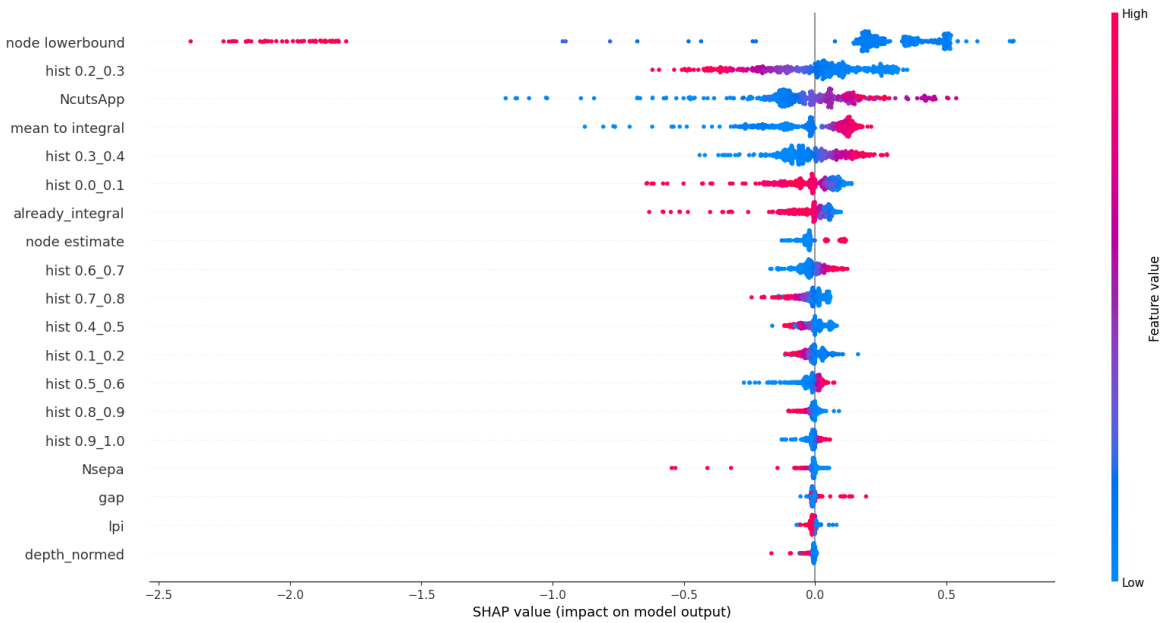


Figure 4: Beeswarm plot showing feature importance of individual nodes using the KernelSHAP (Lundberg & Lee, 2017) method.

methods were trained against older versions of SCIP, which not only made running them challenging, but also would not give valid comparisons as we cannot properly account for changes between SCIP versions. Labassi et al. (2022) specifically relies on changes to the SCIP interface, which makes porting to SCIP 8.0.4 intractable. In general, this shouldn't matter too much, as SCIP is still demonstrably the state-of-the-art non-commercial mixed-integer solver, which frequently outperforms even closed-source commercial solvers (see Mittelman (2021) for thorough benchmarks against other solvers), meaning outperforming SCIP can be seen as outperforming the state-of-the-art.

I.1 Kochetov-UFLP

To demonstrate the generalizability of the learned heuristics, we test our method on the Uncapacitated Facility Location Problem (see Appendix G) *without further finetuning*, i.e., we only train on TSP instances and never show the algorithm any other linear or nonlinear problem. For testing, we generate 1000 instances using the well-known problem generator by Kochetov & Ivanenko (2005), which was designed to have large optimality gaps, making these problems particularly challenging.

Our method performs very similar to the highly optimized baseline, despite never having seen the UFL problem, see Table 1. We argue that this is specifically because our method relies on tree-wide behaviour, rather than individual features to make decisions. We further hypothesize that the reason for the advantage over the baseline being so small is due to the fact that UFLP consists of “adversarial examples” to the branch-and-bound method where cuts have reduced effectiveness. This means clever node-selection strategies have limited impact on overall performance.

An interesting aspect is that our method processes more nodes than the baseline, which also leads to the loss in node-efficiency. This implies that our method selects significantly easier nodes, as ordinarily our solver is slower just due to the additional overhead. Considering that this benchmark was specifically designed to produce high optimality gaps, it makes sense that our solver favours node quantity over quality, which is an interesting emergent behaviour of our solver.

I.2 TSPLIB results

Table 6: Results on TSPLIB (Reinelt, 1991) after 45s runtime. Note that we filter out problems in which less than 5 nodes were explored as those problems cannot gain meaningful advantages even with perfect node selection. “Name” refers to the instances name, “Gap Base/Ours” corresponds to the optimization gap achieved by the baseline and our method respectively (lower is better), “Nodes Base/Ours” to the number of explored Nodes by each method, and “Reward”, “Utility” and “Utility Node” to the different performance measures as described in Section 5.

Name	Gap Ours	Gap Base	Nodes Ours	Nodes Base	Reward	Utility	Utility/Node
att48	0.287	0.286	1086	2670	-0.002	-0.002	0.593
bayg29	0.000	0.000	2317	7201	1.000	0.000	0.000
bays29	0.000	0.036	11351	10150	1.000	1.000	0.997
berlin52	0.000	0.000	777	1634	1.000	0.000	0.000
bier127	2.795	2.777	23	25	-0.007	-0.007	0.074
brazil58	0.328	0.644	1432	2182	0.491	0.491	0.666
burma14	0.000	0.000	96	65	1.000	0.000	0.000
ch130	8.801	8.783	48	43	-0.002	-0.002	-0.106
ch150	7.803	7.802	18	18	-0.000	-0.000	-0.000
d198	0.582	0.582	10	11	-0.000	-0.000	0.091
dantzig42	0.185	0.100	2498	3469	-0.847	-0.459	-0.248
eil101	2.434	2.430	31	61	-0.002	-0.002	0.491
eil51	0.178	0.017	828	4306	-1.000	-0.907	-0.514
eil76	0.432	1.099	309	709	0.607	0.607	0.829
fri26	0.000	0.000	1470	6721	1.000	0.000	0.000
gr120	7.078	7.083	41	43	0.001	0.001	0.047
gr137	0.606	0.603	30	25	-0.006	-0.006	-0.171
gr17	0.000	0.000	92	123	1.000	0.000	0.000
gr24	0.000	0.000	110	207	1.000	0.000	0.000
gr48	0.192	0.340	586	2479	0.435	0.435	0.866
gr96	0.569	0.552	93	182	-0.032	-0.031	0.472
hk48	0.071	0.106	2571	2990	0.324	0.324	0.419
kroA100	8.937	8.945	102	233	0.001	0.001	0.563
kroA150	11.343	11.340	23	21	-0.000	-0.000	-0.087
kroA200	13.726	13.723	5	7	-0.000	-0.000	0.286
kroB100	7.164	7.082	83	109	-0.011	-0.011	0.230
kroB150	10.965	10.965	16	14	0.000	0.000	-0.125
kroB200	11.740	11.740	7	6	0.000	0.000	-0.143
kroC100	8.721	8.754	118	133	0.004	0.004	0.116
kroD100	7.959	7.938	70	111	-0.003	-0.003	0.368
kroE100	8.573	2.952	105	108	-1.000	-0.656	-0.646
lin105	2.005	2.003	98	149	-0.001	-0.001	0.341
pr107	1.367	1.336	128	217	-0.024	-0.023	0.396
pr124	0.937	0.935	64	61	-0.001	-0.001	-0.048
pr136	2.351	2.350	31	45	-0.000	-0.000	0.311
pr144	2.228	2.200	47	37	-0.012	-0.012	-0.222
pr152	2.688	2.683	14	41	-0.002	-0.002	0.658
pr226	1.091	1.092	6	6	0.001	0.001	0.001
pr76	0.534	0.476	201	855	-0.123	-0.109	0.736
rat99	0.853	0.849	41	80	-0.005	-0.005	0.485
rd100	5.948	4.462	100	166	-0.333	-0.250	0.197
si175	0.270	0.270	8	7	0.000	0.000	-0.125
st70	0.586	3.018	379	1068	0.806	0.806	0.931
swiss42	0.000	0.000	1075	1133	1.000	0.000	0.000
ulysses16	0.000	0.000	18322	19553	1.000	0.000	0.000
ulysses22	0.103	0.127	13911	13313	0.191	0.191	0.154
Mean	—	—	1321	1799	0.184	0.030	0.193

I.3 MIPLIB results

Table 7: Results on MIPLIB (Gleixner et al., 2021) after 45s runtime. Note that we filter out problems in which less than 5 nodes were explored as those problems cannot gain meaningful advantages even with perfect node selection. “Name” refers to the instances name, “Gap Base/Ours” corresponds to the optimization gap achieved by the baseline and our method respectively (lower is better), “Nodes Base/Ours” to the number of explored Nodes by each method, and “Reward”, “Utility” and “Utility Node” to the different performance measures as described in Section 5. Note that all results were achieved with a policy only trained on TSP instances

Name	Gap Ours	Gap Base	Nodes Ours	Nodes Base	Reward	Utility	Utility/Node
30n20b8	2.662	∞	147	301	1.000	1.000	1.000
50v-10	0.101	0.113	303	1094	0.103	0.103	0.752
CMS750_4	0.100	0.072	68	281	-0.389	-0.280	0.664
air05	0.000	0.000	248	523	1.000	0.000	0.000
assign1-5-8	0.085	0.087	17466	23589	0.030	0.030	0.282
binkar10_1	0.000	0.000	2843	2270	1.000	0.000	0.000
blp-ic98	0.127	0.127	26	43	0.001	0.001	0.396
bnatt400	∞	∞	547	1568	0.000	0.000	0.651
bnatt500	∞	∞	148	936	0.000	0.000	0.842
bppc4-08	0.038	0.038	1318	3277	0.000	0.000	0.598
cost266-UUE	0.130	0.143	468	770	0.094	0.094	0.449
csched007	∞	∞	558	1770	0.000	0.000	0.685
csched008	0.070	∞	910	1179	1.000	1.000	1.000
cvs16r128-89	0.560	0.601	6	7	0.068	0.068	0.202
drayage-25-23	0.000	0.000	105	267	1.000	0.000	0.000
dws008-01	∞	∞	123	173	0.000	0.000	0.289
eil33-2	0.194	0.189	191	171	-0.025	-0.024	-0.127
fast0507	0.027	0.027	11	7	-0.003	-0.003	-0.366
fastxgemm-n2r6s0t2	18.519	18.519	785	2531	0.000	0.000	0.690
fhnw-binpack4-4	∞	∞	140002	152608	0.000	0.000	0.083
fhnw-binpack4-48	∞	0.000	15019	24649	-1.000	-1.000	-1.000
fiball	0.029	0.036	442	610	0.200	0.200	0.420
gen-ip002	0.008	0.010	88794	125319	0.197	0.197	0.397
gen-ip054	0.008	0.010	157950	179874	0.207	0.207	0.263
glass-sc	0.580	0.495	200	328	-0.173	-0.148	0.285
glass4	1.123	1.033	37424	35671	-0.087	-0.080	-0.123
gmu-35-40	0.001	0.001	28534	27077	0.402	0.398	0.276
gmu-35-50	0.001	0.001	16456	22333	0.177	0.176	0.346
graph20-20-1rand	0.000	0.000	416	283	1.000	0.000	0.000
graphdraw-domain	0.421	0.430	49640	56798	0.022	0.022	0.145
ic97_potential	0.023	0.040	39316	30633	0.415	0.415	0.247
icir97_tension	0.011	0.006	6697	7943	-0.882	-0.468	-0.367
irp	0.000	0.000	6	6	1.000	0.000	0.000
istanbul-no-cutoff	0.514	0.393	37	28	-0.309	-0.236	-0.422
lectsched-5-obj	∞	2.200	1192	1118	-1.000	-1.000	-1.000
leo1	0.118	0.113	34	108	-0.049	-0.046	0.670
leo2	0.345	0.135	49	61	-1.000	-0.609	-0.514
mad	∞	∞	78783	81277	0.000	0.000	0.031
markshare2	∞	∞	91135	127265	0.000	0.000	0.284
markshare_4_0	∞	∞	570277	682069	0.000	0.000	0.164
mas74	0.079	0.084	32005	26180	0.060	0.060	-0.129
mas76	0.014	0.015	49987	52401	0.060	0.060	0.100
mc11	0.008	0.009	333	1989	0.139	0.138	0.855
mcsched	0.090	0.086	439	1526	-0.049	-0.046	0.698
mik-250-20-75-4	0.000	0.000	10067	10120	1.000	0.000	0.000
milov12-6-r2-40-1	0.038	0.031	340	514	-0.242	-0.195	0.179
momentum1	2.868	2.868	10	9	-0.000	-0.000	-0.100
n2seq36q	0.665	0.665	5	6	0.000	0.000	0.167
n5-3	0.046	0.000	427	595	-1.000	-1.000	-1.000
neos-1171737	0.032	0.032	7	13	0.000	0.000	0.462
neos-1445765	0.000	0.000	190	263	1.000	0.000	0.000
neos-1456979	∞	0.344	204	405	-1.000	-1.000	-1.000
neos-1582420	0.016	0.016	11	11	0.000	0.000	0.000
neos-2657525-crna	∞	∞	42826	45188	0.000	0.000	0.052
neos-2978193-inde	0.013	0.013	964	2178	0.000	0.000	0.557
neos-3004026-krka	∞	∞	1134	1163	0.000	0.000	0.025
neos-3024952-loue	∞	∞	246	377	0.000	0.000	0.347
neos-3046615-murg	2.515	2.631	66921	79117	0.044	0.044	0.191
neos-3083819-nubu	0.000	0.000	1683	1687	1.000	0.000	0.000
neos-3381206-awhea	0.000	0.000	969	230	1.000	0.000	0.000
neos-3402294-bobin	∞	∞	10	24	0.000	0.000	0.583
neos-3627168-kasai	0.003	0.008	6269	3338	0.577	0.577	0.205

Continued on next page

Name	Gap Ours	Gap Base	Nodes Ours	Nodes Base	Reward	Utility	Utility/Node
neos-3754480-nidda	∞	∞	87703	106632	0.000	0.000	0.178
neos-4338804-snowy	0.024	0.028	37447	36741	0.125	0.125	0.107
neos-4387871-tavua	0.631	0.634	5	7	0.005	0.005	0.289
neos-4738912-atrato	0.016	0.006	529	1064	-1.000	-0.634	-0.265
neos-4954672-berkel	0.265	0.254	454	775	-0.043	-0.041	0.389
neos-5093327-huahum	0.539	0.559	5	6	0.036	0.036	0.197
neos-5107597-kakapo	2.639	5.077	1885	2332	0.480	0.480	0.580
neos-5188808-nattai	∞	∞	16	105	0.000	0.000	0.848
neos-5195221-niemur	106.417	106.417	11	12	0.000	0.000	0.083
neos-911970	0.000	0.000	3905	15109	1.000	0.000	0.000
neos17	0.000	0.000	2151	3346	1.000	0.000	0.000
neos5	0.062	0.059	66231	91449	-0.053	-0.050	0.235
neos859080	0.000	0.000	990	1227	1.000	0.000	0.000
net12	2.592	2.114	56	29	-0.227	-0.185	-0.578
ns1208400	∞	∞	82	150	0.000	0.000	0.453
ns1830653	2.831	1.242	334	686	-1.000	-0.561	-0.099
ns1952667	∞	∞	100	52	0.000	0.000	-0.480
nu25-pr12	0.000	0.000	119	153	1.000	0.000	0.000
nursesched-sprint02	0.000	0.000	9	7	1.000	0.000	0.000
nw04	0.000	0.000	6	6	1.000	0.000	0.000
pg	0.000	0.000	460	491	1.000	0.000	0.000
pg5_34	0.004	0.004	275	592	-0.023	-0.022	0.524
piperout-08	0.000	0.000	223	309	1.000	0.000	0.000
piperout-27	0.000	0.000	47	28	1.000	0.000	0.000
pk1	1.244	1.117	102268	120685	-0.113	-0.102	0.057
radiationm18-12-05	0.057	0.167	886	2569	0.661	0.661	0.883
rail507	0.033	0.033	10	9	0.000	0.000	-0.100
ran14x18-disj-8	0.115	0.092	458	975	-0.251	-0.200	0.412
rd-rplusc-21	∞	∞	137	3542	0.000	0.000	0.961
reblock115	0.106	0.139	80	731	0.238	0.238	0.917
rmatr100-p10	0.216	0.326	43	74	0.337	0.337	0.615
rocI-4-11	0.671	0.837	12054	7909	0.198	0.198	-0.181
rocII-5-11	3.479	1.568	164	287	-1.000	-0.549	-0.211
rococoB10-011000	1.244	1.258	12	26	0.012	0.012	0.544
rococoC10-001000	0.337	0.153	135	866	-1.000	-0.546	0.656
roll3000	0.000	0.000	1156	2046	1.000	0.000	0.000
sct2	0.001	0.002	2117	1215	0.619	0.615	0.332
seymour	0.044	0.035	176	563	-0.243	-0.195	0.611
seymour1	0.003	0.003	329	885	0.146	0.145	0.682
sp150x300d	0.000	0.000	148	124	1.000	0.000	0.000
supportcase18	0.081	0.081	178	1372	0.000	-0.000	0.870
supportcase26	0.224	0.231	11191	20287	0.031	0.031	0.465
supportcase33	27.788	0.371	15	28	-1.000	-0.987	-0.975
supportcase40	0.086	0.094	50	111	0.087	0.087	0.589
supportcase42	0.033	0.050	76	256	0.340	0.340	0.804
swath1	0.000	0.000	311	372	1.000	0.000	0.000
swath3	0.110	0.113	1442	2800	0.020	0.020	0.495
timtab1	0.126	0.094	22112	25367	-0.333	-0.250	-0.139
tr12-30	0.002	0.002	8941	14896	0.019	0.019	0.394
traininstance2	∞	∞	412	821	0.000	0.000	0.498
traininstance6	29.355	∞	2549	6376	1.000	1.000	1.000
trento1	3.885	3.885	4	7	-0.000	-0.000	0.429
uct-subprob	0.249	0.195	225	263	-0.276	-0.216	-0.084
var-smallemary-m6j6	0.062	0.062	95	224	-0.002	-0.002	0.575
wachplan	0.125	0.125	422	712	0.000	0.000	0.407
Mean	—	—	16538	19673	0.140	-0.013	0.208

I.4 MINLPLIB results

Table 8: Results on MINLPLIB (Bussieck et al., 2003) after 45s runtime. Note that we filter out problems in which less than 5 nodes were explored as those problems cannot gain meaningful advantages even with perfect node selection. “Name” refers to the instances name, “Gap Base/Ours” corresponds to the optimization gap achieved by the baseline and our method respectively (lower is better), “Nodes Base/Ours” to the number of explored Nodes by each method, and “Reward”, “Utility” and “Utility Node” to the different performance measures as described in Section 5. For all three measures, higher is better.

Name	Gap Ours	Gap Base	Nodes Ours	Nodes Base	Reward	Utility	Utility/Node
ball_mk4_05	0.000	0.000	1819	1869	1.000	0.000	0.000

Continued on next page

Name	Gap Ours	Gap Base	Nodes Ours	Nodes Base	Reward	Utility	Utility/Node
ball_mk4_10	∞	∞	31684	37656	0.000	0.000	0.159
ball_mk4_15	∞	∞	1773	2415	0.000	0.000	0.266
bayes2_20	∞	∞	3171	2719	0.000	0.000	-0.143
bayes2_30	∞	∞	4462	4992	0.000	0.000	0.106
bayes2_50	∞	∞	2934	2530	0.000	0.000	-0.138
blend029	0.000	0.000	812	804	1.000	0.000	0.000
blend146	0.097	0.105	12390	18066	0.075	0.075	0.365
blend480	0.071	0.000	4878	6312	-1.000	-1.000	-0.999
blend531	0.000	0.000	3150	7161	1.000	0.000	0.000
blend718	0.898	0.796	22652	26060	-0.127	-0.113	0.020
blend721	0.000	0.000	4650	2708	1.000	0.000	0.000
blend852	0.021	0.000	7726	5413	-1.000	-1.000	-0.997
camshape100	0.076	0.074	18839	22205	-0.027	-0.026	0.128
camshape200	0.145	0.147	8199	9921	0.012	0.012	0.183
camshape400	0.198	0.195	4324	5275	-0.016	-0.016	0.167
camshape800	0.222	0.226	1504	1627	0.019	0.019	0.093
cardqp_inlp	1.436	1.660	4316	7232	0.135	0.135	0.484
cardqp_iqp	1.089	1.660	4766	7285	0.344	0.344	0.571
carton7	0.000	0.000	55	73	1.000	0.000	0.000
carton9	0.000	0.000	9848	7406	1.000	0.000	0.000
catmix100	∞	∞	186	8750	0.000	0.000	0.979
catmix200	∞	∞	123	3870	0.000	0.000	0.968
catmix400	∞	∞	146	3498	0.000	0.000	0.958
catmix800	∞	∞	75	333	0.000	0.000	0.775
celar6-sub0	∞	∞	4	6	0.000	0.000	0.333
chimera_k64ising-01	0.701	16.469	18	21	0.957	0.957	0.964
chimera_k64maxcut-01	0.523	0.199	57	198	-1.000	-0.618	0.246
chimera_k64maxcut-02	0.368	0.239	72	381	-0.536	-0.349	0.710
chimera_lga-02	0.893	0.893	5	6	0.000	0.000	0.167
chimera_mgw-c8-439-onc8-001	0.045	0.021	127	521	-1.000	-0.529	0.482
chimera_mgw-c8-439-onc8-002	0.067	0.046	72	526	-0.449	-0.310	0.802
chimera_mgw-c8-507-onc8-01	0.232	0.233	26	99	0.003	0.003	0.738
chimera_mgw-c8-507-onc8-02	0.188	0.346	14	25	0.455	0.455	0.695
chimera_mis-01	0.000	0.000	7	7	1.000	0.000	0.000
chimera_mis-02	0.000	0.000	7	7	1.000	0.000	0.000
chimera_rfr-01	1.029	1.153	70	61	0.108	0.108	-0.023
chimera_rfr-02	1.148	1.061	74	63	-0.082	-0.076	-0.213
chimera_selby-c8-onc8-01	0.436	0.224	34	111	-0.941	-0.485	0.406
chimera_selby-c8-onc8-02	0.439	0.232	40	92	-0.895	-0.472	0.176
clay0203m	0.000	0.000	19	30	1.000	0.000	0.000
clay0204m	0.000	0.000	266	400	1.000	0.000	0.000
clay0205m	0.000	0.000	4058	3908	1.000	0.000	0.000
clay0303m	0.000	0.000	107	45	1.000	0.000	0.000
clay0304m	0.000	0.000	337	897	1.000	0.000	0.000
clay0305m	0.000	0.000	4057	4204	1.000	0.000	0.000
color_lab3_3x0	1.445	1.725	320	576	0.162	0.162	0.534
color_lab3_4x0	5.581	5.455	265	434	-0.023	-0.023	0.375
crossdock_15x7	4.457	8.216	654	1080	0.458	0.458	0.672
crossdock_15x8	8.578	84.148	391	717	0.898	0.898	0.944
crudeoil_lee1_06	0.000	0.000	48	57	1.000	0.000	0.000
crudeoil_lee1_07	0.000	0.000	57	92	1.000	0.000	0.000
crudeoil_lee1_08	0.000	0.000	161	121	1.000	0.000	0.000
crudeoil_lee1_09	0.000	0.000	107	99	1.000	0.000	0.000
crudeoil_lee1_10	0.000	0.000	78	109	1.000	0.000	0.000
crudeoil_lee2_05	0.000	0.000	10	11	1.000	0.000	0.000
crudeoil_lee2_06	0.000	0.000	45	109	1.000	0.000	0.000
crudeoil_lee2_07	0.000	0.000	286	81	1.000	0.000	0.000
crudeoil_lee2_08	0.000	0.000	150	308	1.000	0.000	0.000
crudeoil_lee2_09	0.142	0.015	44	41	-1.000	-0.897	-0.904
crudeoil_lee3_05	0.000	0.000	1435	1820	1.000	0.000	0.000
crudeoil_lee3_06	0.057	0.013	352	1349	-1.000	-0.764	-0.095
crudeoil_lee4_05	0.000	0.000	306	118	1.000	0.000	0.000
crudeoil_lee4_06	0.000	0.000	129	60	1.000	0.000	0.000
crudeoil_lee4_07	0.000	0.000	193	89	1.000	0.000	0.000
crudeoil_lee4_08	0.000	0.001	41	53	0.187	0.184	0.371
crudeoil_li01	0.049	0.017	16819	11797	-1.000	-0.657	-0.758
crudeoil_li02	0.013	0.013	12172	10426	-0.027	-0.027	-0.165
crudeoil_li03	∞	∞	198	899	0.000	0.000	0.780
crudeoil_li05	0.157	0.142	553	1031	-0.104	-0.095	0.408
crudeoil_li06	∞	∞	41	322	0.000	0.000	0.873
crudeoil_li11	∞	∞	20	70	0.000	0.000	0.714
crudeoil_pooling_ct1	0.943	0.988	2415	6356	0.046	0.046	0.638
crudeoil_pooling_ct2	0.000	0.000	1480	1589	1.000	0.000	0.000
crudeoil_pooling_ct3	42.222	120.618	101	101	0.650	0.650	0.650
crudeoil_pooling_ct4	0.000	0.000	7631	9217	0.365	0.153	0.041
du-opt	0.000	0.000	11282	14174	1.000	0.000	0.000
du-opt5	0.000	0.000	83	60	1.000	0.000	0.000

Continued on next page

Name	Gap Ours	Gap Base	Nodes Ours	Nodes Base	Reward	Utility	Utility/Node
edgexcross10-030	0.000	0.000	7	7	1.000	0.000	0.000
edgexcross10-040	0.000	0.000	30	39	1.000	0.000	0.000
edgexcross10-050	0.000	0.000	487	469	1.000	0.000	0.000
edgexcross10-060	0.000	0.000	2058	2138	1.000	0.000	0.000
edgexcross10-070	0.321	0.220	255	329	-0.457	-0.314	-0.115
edgexcross10-080	0.077	0.077	352	668	0.001	0.001	0.474
edgexcross10-090	0.000	0.000	7	6	1.000	0.000	0.000
edgexcross14-039	0.000	0.000	624	731	1.000	0.000	0.000
edgexcross14-058	1.251	0.549	84	157	-1.000	-0.561	-0.180
edgexcross14-078	1.843	1.865	12	14	0.012	0.012	0.153
edgexcross14-098	1.120	1.129	24	31	0.007	0.007	0.232
edgexcross14-117	0.963	0.947	9	17	-0.017	-0.017	0.462
edgexcross14-137	0.537	0.552	20	30	0.028	0.028	0.352
edgexcross14-156	0.338	0.353	13	13	0.042	0.042	0.042
edgexcross14-176	0.089	0.080	37	135	-0.117	-0.105	0.694
edgexcross20-040	0.000	0.000	71	57	1.000	0.000	0.000
edgexcross20-080	3.943	3.943	7	7	0.000	0.000	0.000
edgexcross22-048	0.615	0.000	56	81	-1.000	-1.000	-1.000
edgexcross24-057	5.219	5.219	7	6	0.000	0.000	-0.143
elf	0.000	0.000	115	112	1.000	0.000	0.000
ex2_1_1	0.000	0.000	17	17	1.000	0.000	0.000
ex2_1_10	0.000	0.000	13	11	1.000	0.000	0.000
ex2_1_5	0.000	0.000	17	19	1.000	0.000	0.000
ex2_1_6	0.000	0.000	13	13	1.000	0.000	0.000
ex2_1_7	0.000	0.000	1523	1831	1.000	0.000	0.000
ex2_1_8	0.000	0.000	75	93	1.000	0.000	0.000
ex2_1_9	0.000	0.000	3735	3947	1.000	0.000	0.000
ex3_1_1	0.000	0.000	405	271	1.000	0.000	0.000
ex3_1_3	0.000	0.000	21	27	1.000	0.000	0.000
ex3_1_4	0.000	0.000	23	23	1.000	0.000	0.000
ex4	0.000	0.000	23	29	1.000	0.000	0.000
ex5_2_2_case1	0.000	0.000	39	19	1.000	0.000	0.000
ex5_2_2_case2	0.000	0.000	57	31	1.000	0.000	0.000
ex5_2_4	0.000	0.000	251	227	1.000	0.000	0.000
ex5_2_5	0.359	0.346	30403	33492	-0.038	-0.036	0.058
ex5_3_2	0.000	0.000	33	31	1.000	0.000	0.000
ex5_3_3	0.339	0.331	29464	31558	-0.024	-0.024	0.044
ex5_4_2	0.000	0.000	41	35	1.000	0.000	0.000
ex8_3_2	23.252	23.608	8907	8680	0.015	0.015	-0.011
ex8_3_3	23.004	23.004	9636	10365	0.000	0.000	0.070
ex8_3_4	1.817	1.793	9447	9563	-0.013	-0.013	-0.001
ex8_3_5	143.677	143.677	9427	9699	0.000	0.000	0.028
ex8_3_8	2.071	2.071	2293	3677	0.000	0.000	0.376
ex8_3_9	12.106	12.106	14272	17310	0.000	-0.000	0.176
ex8_4_1	0.000	0.000	670	650	1.000	0.000	0.000
ex9_2_3	0.000	0.000	25	31	1.000	0.000	0.000
ex9_2_5	0.000	0.000	27	29	1.000	0.000	0.000
ex9_2_7	0.000	0.000	11	11	1.000	0.000	0.000
faclay20h	1.727	1.727	16	15	0.000	0.000	-0.062
faclay25	2.468	2.468	6	6	0.000	0.000	0.000
forest	0.003	0.020	29002	25913	0.860	0.859	0.831
gabriel01	0.139	0.139	6753	9744	-0.000	-0.000	0.307
gabriel02	0.556	0.585	1107	1675	0.050	0.050	0.372
gabriel04	∞	1.308	129	285	-1.000	-1.000	-1.000
gabriel05	∞	∞	141	326	0.000	0.000	0.567
gasprod_sarawak01	0.000	0.000	11	6	1.000	0.000	0.000
gasprod_sarawak16	0.004	0.009	506	1052	0.585	0.585	0.800
genpooling_lee1	0.000	0.000	690	676	1.000	0.000	0.000
genpooling_lee2	0.000	0.000	1299	2989	1.000	0.000	0.000
genpooling_meyer04	0.957	0.691	12855	17889	-0.385	-0.278	0.005
genpooling_meyer10	1.276	1.385	1910	2815	0.078	0.078	0.375
genpooling_meyer15	6.080	0.691	97	413	-1.000	-0.886	-0.516
graphpart_2g-0099-9211	0.000	0.000	18	14	1.000	0.000	0.000
graphpart_2pm-0077-0777	0.000	0.000	5	6	1.000	0.000	0.000
graphpart_2pm-0088-0888	0.000	0.000	9	7	1.000	0.000	0.000
graphpart_2pm-0099-0999	0.000	0.000	16	12	1.000	0.000	0.000
graphpart_3g-0334-0334	0.000	0.000	21	41	1.000	0.000	0.000
graphpart_3g-0344-0344	0.000	0.000	61	19	1.000	0.000	0.000
graphpart_3g-0444-0444	0.000	0.000	424	562	1.000	0.000	0.000
graphpart_3pm-0244-0244	0.000	0.000	21	15	1.000	0.000	0.000
graphpart_3pm-0334-0334	0.000	0.000	20	38	1.000	0.000	0.000
graphpart_3pm-0344-0344	0.000	0.000	590	619	1.000	0.000	0.000
graphpart_3pm-0444-0444	0.058	0.000	755	1348	-1.000	-1.000	-1.000
graphpart_clique-20	0.000	0.000	22	24	1.000	0.000	0.000
graphpart_clique-30	0.000	0.000	421	337	1.000	0.000	0.000
graphpart_clique-40	1.018	0.920	297	609	-0.106	-0.096	0.461
graphpart_clique-50	5.638	6.032	97	191	0.065	0.065	0.525

Continued on next page

Name	Gap Ours	Gap Base	Nodes Ours	Nodes Base	Reward	Utility	Utility/Node
graphpart_clique-60	17.434	9.335	109	204	-0.868	-0.465	0.002
graphpart_clique-70	30.409	35.053	16	27	0.132	0.132	0.486
haverly	0.000	0.000	45	57	1.000	0.000	0.000
himmel16	0.000	0.000	2193	2089	1.000	0.000	0.000
house	0.000	0.000	58675	58399	1.000	0.000	0.000
hvb11	0.018	0.182	19172	15631	0.899	0.899	0.875
hydroenergy1	0.007	0.007	15060	18149	-0.088	-0.081	0.095
hydroenergy2	0.016	0.016	4834	6712	0.038	0.038	0.306
hydroenergy3	0.022	0.023	565	1060	0.006	0.006	0.470
ising2_5-300_5555	0.508	0.407	57	220	-0.248	-0.199	0.677
kall_circles_c6a	3.180	2.094	42813	46497	-0.519	-0.342	-0.285
kall_circles_c6b	2.635	1.452	38722	45596	-0.815	-0.449	-0.351
kall_circles_c6c	∞	∞	33357	36374	0.000	0.000	0.083
kall_circles_c7a	1.482	1.376	38682	43723	-0.077	-0.072	0.047
kall_circles_c8a	∞	∞	32114	36262	0.000	0.000	0.114
kall_circlespolygons_c1p12	0.000	0.000	44439	64102	-1.000	-0.733	-0.106
kall_circlespolygons_c1p13	0.000	0.000	8621	7914	1.000	0.000	0.000
kall_circlespolygons_c1p5a	∞	∞	12369	13200	0.000	0.000	0.063
kall_circlespolygons_c1p6a	∞	∞	404	628	0.000	0.000	0.357
kall_circlesrectangles_clr12	0.000	0.000	42587	48285	0.121	0.114	0.061
kall_circlesrectangles_clr13	0.000	0.000	4372	3739	1.000	0.000	0.000
kall_circlesrectangles_c6r1	∞	∞	5850	7908	0.000	0.000	0.260
kall_circlesrectangles_c6r29	∞	∞	4181	5220	0.000	0.000	0.199
kall_circlesrectangles_c6r39	∞	∞	2570	2966	0.000	0.000	0.134
kall_congruentcircles_c31	0.000	0.000	101	95	1.000	0.000	0.000
kall_congruentcircles_c32	0.000	0.000	133	139	1.000	0.000	0.000
kall_congruentcircles_c41	0.000	0.000	27	31	1.000	0.000	0.000
kall_congruentcircles_c42	0.000	0.000	205	125	1.000	0.000	0.000
kall_congruentcircles_c51	0.000	0.000	4197	4987	1.000	0.000	0.000
kall_congruentcircles_c52	0.000	0.000	1767	1446	1.000	0.000	0.000
kall_congruentcircles_c61	0.000	0.000	27338	35199	1.000	0.000	0.000
kall_congruentcircles_c62	0.000	0.000	2879	6037	1.000	0.000	0.000
kall_congruentcircles_c63	0.000	0.000	2043	1729	1.000	0.000	0.000
kall_congruentcircles_c71	∞	∞	39102	43349	0.000	0.000	0.098
kall_congruentcircles_c72	0.000	0.000	14686	14089	1.000	0.000	0.000
kall_diffcircles_10	2.276	4.054	32475	41241	0.439	0.439	0.558
kall_diffcircles_5a	0.000	0.000	2020	1218	1.000	0.000	0.000
kall_diffcircles_5b	0.000	0.000	6360	5774	1.000	0.000	0.000
kall_diffcircles_6	0.000	0.000	2827	2383	1.000	0.000	0.000
kall_diffcircles_7	0.000	0.000	9408	9518	1.000	0.000	0.000
kall_diffcircles_8	0.406	0.219	48924	57747	-0.851	-0.460	-0.362
kall_diffcircles_9	1.676	1.052	42056	48915	-0.594	-0.373	-0.270
knp3-12	1.846	1.963	1987	2132	0.060	0.060	0.124
lop97ic	∞	∞	19	33	0.000	0.000	0.424
lop97icx	0.008	0.000	3041	1711	-1.000	-0.999	-0.998
maxcsp-langford-3-11	∞	∞	1356	4038	0.000	0.000	0.664
ndcc12	∞	∞	1394	3975	0.000	0.000	0.649
ndcc12persp	∞	∞	1092	2994	0.000	0.000	0.635
ndcc13	∞	∞	298	787	0.000	0.000	0.621
ndcc13persp	0.536	0.546	2982	5662	0.018	0.018	0.483
ndcc14	1.030	1.048	234	499	0.018	0.018	0.539
ndcc14persp	1.044	1.080	572	1052	0.033	0.033	0.474
ndcc15	∞	∞	1293	2120	0.000	0.000	0.390
ndcc15persp	∞	∞	5227	6549	0.000	0.000	0.202
ndcc16	∞	∞	407	396	0.000	0.000	-0.027
ndcc16persp	∞	∞	1035	2183	0.000	0.000	0.526
netmod_dol2	0.047	0.000	112	250	-1.000	-1.000	-1.000
netmod_kar1	0.000	0.000	425	285	1.000	0.000	0.000
netmod_kar2	0.000	0.000	275	285	1.000	0.000	0.000
nous1	0.000	0.000	3092	2816	1.000	0.000	0.000
nous2	0.000	0.000	81	71	1.000	0.000	0.000
nuclearvb	∞	∞	1821	3817	0.000	0.000	0.523
nuclearvc	∞	∞	1905	1530	0.000	0.000	-0.197
nuclearvd	∞	∞	3781	2521	0.000	0.000	-0.333
nuclearve	∞	∞	877	5464	0.000	0.000	0.839
nuclearvf	∞	∞	256	3596	0.000	0.000	0.929
nvs13	0.000	0.000	9	9	1.000	0.000	0.000
nvs17	0.000	0.000	89	78	1.000	0.000	0.000
nvs18	0.000	0.000	121	75	1.000	0.000	0.000
nvs19	0.000	0.000	161	154	1.000	0.000	0.000
nvs23	0.000	0.000	465	523	1.000	0.000	0.000
nvs24	0.000	0.000	2060	1944	1.000	0.000	0.000
p_ball_10b_5p_2d_m	0.000	0.000	353	326	1.000	0.000	0.000
p_ball_10b_5p_3d_m	0.000	0.000	1204	1032	1.000	0.000	0.000
p_ball_10b_5p_4d_m	0.000	0.000	1424	1765	1.000	0.000	0.000
p_ball_10b_7p_3d_m	0.000	0.000	6178	6151	1.000	0.000	0.000
p_ball_15b_5p_2d_m	0.000	0.000	1377	2068	1.000	0.000	0.000

Continued on next page

Name	Gap Ours	Gap Base	Nodes Ours	Nodes Base	Reward	Utility	Utility/Node
p_ball_20b_5p_2d_m	0.000	0.000	1610	2039	1.000	0.000	0.000
p_ball_20b_5p_3d_m	0.000	0.000	10647	11510	1.000	0.000	0.000
p_ball_30b_10p_2d_m	∞	∞	3795	4965	0.000	0.000	0.236
p_ball_30b_5p_2d_m	0.000	0.000	2827	3275	1.000	0.000	0.000
p_ball_30b_5p_3d_m	0.000	0.000	10150	11489	1.000	0.000	0.000
p_ball_30b_7p_2d_m	∞	∞	8511	11906	0.000	0.000	0.285
p_ball_40b_5p_3d_m	∞	∞	9620	13718	0.000	0.000	0.299
p_ball_40b_5p_4d_m	∞	∞	8100	11826	0.000	0.000	0.315
pedigree_ex485	0.019	0.019	315	962	0.030	0.030	0.682
pedigree_ex485_2	0.000	0.000	121	344	1.000	0.000	0.000
pedigree_sim400	0.061	0.053	1094	1533	-0.156	-0.135	0.175
pedigree_sp_top4_250	0.053	0.036	61	173	-0.482	-0.325	0.477
pedigree_sp_top4_300	0.014	0.015	294	670	0.014	0.014	0.567
pedigree_sp_top4_350tr	0.000	0.014	365	1096	1.000	0.999	1.000
pedigree_sp_top5_250	0.050	0.057	28	39	0.125	0.125	0.372
pinene200	∞	∞	12	12	0.000	0.000	0.000
pointpack06	0.000	0.000	2099	2051	1.000	0.000	0.000
pointpack08	0.015	0.000	35620	34315	-1.000	-0.999	-0.978
pointpack10	0.612	0.613	18366	22179	0.001	0.001	0.173
pointpack12	0.854	0.839	15197	17796	-0.018	-0.018	0.131
pointpack14	1.535	1.537	8919	9550	0.001	0.001	0.067
pooling_adhya1pq	0.000	0.000	383	365	1.000	0.000	0.000
pooling_adhya1stp	0.000	0.000	737	638	1.000	0.000	0.000
pooling_adhya1tp	0.000	0.000	611	806	1.000	0.000	0.000
pooling_adhya2pq	0.000	0.000	569	588	1.000	0.000	0.000
pooling_adhya2stp	0.000	0.000	832	934	1.000	0.000	0.000
pooling_adhya2tp	0.000	0.000	345	288	1.000	0.000	0.000
pooling_adhya3pq	0.000	0.000	377	289	1.000	0.000	0.000
pooling_adhya3stp	0.000	0.000	834	1078	1.000	0.000	0.000
pooling_adhya3tp	0.000	0.000	675	585	1.000	0.000	0.000
pooling_adhya4pq	0.000	0.000	274	150	1.000	0.000	0.000
pooling_adhya4stp	0.000	0.000	385	686	1.000	0.000	0.000
pooling_adhya4tp	0.000	0.000	317	387	1.000	0.000	0.000
pooling_bental5stp	0.000	0.000	2818	4434	1.000	0.000	0.000
pooling_digabel16	0.000	0.000	27577	35207	-1.000	-0.715	-0.160
pooling_digabel18	0.013	0.008	4109	5110	-0.496	-0.331	-0.168
pooling_digabel19	0.001	0.001	14953	18095	0.168	0.166	0.267
pooling_foulds2stp	0.000	0.000	36	25	1.000	0.000	0.000
pooling_foulds3stp	0.000	0.000	1084	416	1.000	0.000	0.000
pooling_foulds4stp	0.000	0.000	717	339	1.000	0.000	0.000
pooling_foulds5stp	0.019	0.000	1808	2741	-1.000	-0.999	-0.999
pooling_haverly2stp	0.000	0.000	10	12	1.000	0.000	0.000
pooling_rt2pq	0.000	0.000	237	431	1.000	0.000	0.000
pooling_rt2stp	0.000	0.000	109	195	1.000	0.000	0.000
pooling_rt2tp	0.000	0.000	53	57	1.000	0.000	0.000
pooling_sppa0pq	0.038	0.031	2424	3666	-0.230	-0.187	0.187
pooling_sppa0stp	2.829	2.865	2577	3068	0.012	0.012	0.170
pooling_sppa0tp	0.179	0.183	2804	3623	0.021	0.021	0.242
pooling_sppa5pq	0.037	0.018	709	781	-0.995	-0.499	-0.448
pooling_sppa5stp	3.959	3.959	220	278	0.000	0.000	0.209
pooling_sppa5tp	1.579	1.579	299	448	0.000	0.000	0.333
pooling_sppa9pq	0.007	0.007	222	295	0.000	0.000	0.247
pooling_sppb0pq	0.098	0.098	223	301	0.000	-0.000	0.259
popdynm100	∞	∞	7556	11105	0.000	0.000	0.320
popdynm25	∞	∞	14627	19046	0.000	0.000	0.232
popdynm50	∞	∞	12085	15252	0.000	0.000	0.208
portfol_classical050_1	0.000	0.000	651	817	1.000	0.000	0.000
portfol_classical200_2	0.141	0.125	396	491	-0.134	-0.118	0.086
portfol_robust050_34	0.000	0.000	94	49	1.000	0.000	0.000
portfol_robust100_09	0.000	0.000	489	361	1.000	0.000	0.000
portfol_robust200_03	0.182	0.189	95	75	0.034	0.034	-0.183
portfol_shortfall050_68	0.000	0.000	467	375	1.000	0.000	0.000
portfol_shortfall100_04	0.010	0.010	595	1398	-0.055	-0.052	0.551
portfol_shortfall200_05	0.033	0.028	224	232	-0.169	-0.145	-0.114
powerflow0009r	0.000	0.000	15230	13141	-1.000	-0.037	-0.003
powerflow0014r	0.001	0.001	8052	8041	0.368	0.366	0.346
powerflow0030r	0.023	0.034	369	403	0.328	0.328	0.384
powerflow0039r	0.017	0.016	212	224	-0.058	-0.054	-0.001
product	0.028	0.034	236	650	0.197	0.197	0.708
qap	198.418	∞	709	3352	1.000	1.000	1.000
qapw	351.271	∞	874	2437	1.000	1.000	1.000
qp3	∞	∞	29875	32155	0.000	0.000	0.071
qspp_0_10_0_1_10_1	0.849	1.238	3860	3982	0.314	0.314	0.335
qspp_0_11_0_1_10_1	1.071	1.886	1314	3036	0.432	0.432	0.754
qspp_0_12_0_1_10_1	1.674	2.102	794	1847	0.204	0.203	0.658
qspp_0_13_0_1_10_1	1.893	4.660	935	1380	0.594	0.594	0.725
qspp_0_14_0_1_10_1	3.038	3.200	299	1081	0.050	0.050	0.737

Continued on next page

Name	Gap Ours	Gap Base	Nodes Ours	Nodes Base	Reward	Utility	Utility/Node
qspp_0_15_0_1_10_1	4.356	4.293	229	544	-0.015	-0.015	0.573
ringpack_10_1	0.082	1.000	5346	6348	0.918	0.918	0.931
ringpack_10_2	0.082	0.811	5402	6366	0.899	0.899	0.914
ringpack_20_1	1.551	3.527	525	492	0.560	0.560	0.531
ringpack_20_2	9.000	9.000	239	183	0.000	0.000	-0.234
ringpack_20_3	6.251	6.251	272	243	0.000	0.000	-0.107
ringpack_30_2	14.000	14.000	36	49	0.000	0.000	0.265
sep1	0.000	0.000	39	29	1.000	0.000	0.000
slay04h	0.000	0.000	8	8	1.000	0.000	0.000
slay04m	0.000	0.000	7	7	1.000	0.000	0.000
slay05h	0.000	0.000	64	119	1.000	0.000	0.000
slay06h	0.000	0.000	120	208	1.000	0.000	0.000
slay06m	0.000	0.000	8	8	1.000	0.000	0.000
slay07h	0.000	0.000	420	952	1.000	0.000	0.000
slay07m	0.000	0.000	218	501	1.000	0.000	0.000
slay08h	0.000	0.000	513	1181	1.000	0.000	0.000
slay08m	0.000	0.000	193	554	1.000	0.000	0.000
slay09h	0.104	0.135	612	488	0.229	0.229	0.033
slay09m	0.000	0.000	324	212	1.000	0.000	0.000
slay10h	0.103	0.407	703	451	0.746	0.745	0.603
slay10m	0.000	0.000	3933	4138	1.000	0.000	0.000
smallinvDAXr1b010-011	0.000	0.000	324	264	1.000	0.000	0.000
smallinvDAXr1b020-022	0.000	0.000	657	906	1.000	0.000	0.000
smallinvDAXr1b050-055	0.000	0.000	6083	4430	1.000	0.000	0.000
smallinvDAXr1b100-110	0.000	0.000	15366	34917	1.000	0.000	0.000
smallinvDAXr1b150-165	0.000	0.001	26952	40900	1.000	0.986	0.730
smallinvDAXr1b200-220	0.000	0.001	38238	46021	0.348	0.342	0.269
smallinvDAXr2b010-011	0.000	0.000	254	358	1.000	0.000	0.000
smallinvDAXr2b020-022	0.000	0.000	1204	2016	1.000	0.000	0.000
smallinvDAXr2b050-055	0.000	0.000	7868	6682	1.000	0.000	0.000
smallinvDAXr2b100-110	0.000	0.000	12971	14333	1.000	0.000	0.000
smallinvDAXr2b150-165	0.000	0.000	39670	68543	1.000	0.966	0.421
smallinvDAXr2b200-220	0.000	0.000	712	651	1.000	0.000	0.000
smallinvDAXr3b010-011	0.000	0.000	260	358	1.000	0.000	0.000
smallinvDAXr3b020-022	0.000	0.000	1676	906	1.000	0.000	0.000
smallinvDAXr3b050-055	0.000	0.000	5716	5024	1.000	0.000	0.000
smallinvDAXr3b100-110	0.000	0.000	39948	13726	1.000	0.000	0.000
smallinvDAXr3b150-165	0.000	0.000	34109	22132	1.000	0.000	0.000
smallinvDAXr3b200-220	0.000	0.000	1078	433	1.000	0.000	0.000
smallinvDAXr4b010-011	0.000	0.000	272	292	1.000	0.000	0.000
smallinvDAXr4b020-022	0.000	0.000	1078	990	1.000	0.000	0.000
smallinvDAXr4b050-055	0.000	0.000	3098	2666	1.000	0.000	0.000
smallinvDAXr4b100-110	0.000	0.000	17899	26316	1.000	0.000	0.000
smallinvDAXr4b150-165	0.000	0.000	32042	56419	1.000	0.000	0.000
smallinvDAXr4b200-220	0.000	0.000	935	612	1.000	0.000	0.000
smallinvDAXr5b010-011	0.000	0.000	242	381	1.000	0.000	0.000
smallinvDAXr5b020-022	0.000	0.000	1798	884	1.000	0.000	0.000
smallinvDAXr5b050-055	0.000	0.000	4276	3312	1.000	0.000	0.000
smallinvDAXr5b100-110	0.000	0.000	37028	72501	1.000	0.980	0.570
smallinvDAXr5b150-165	0.000	0.000	40757	78031	1.000	0.966	0.414
smallinvDAXr5b200-220	0.000	0.000	783	585	1.000	0.000	0.000
sonet22v5	3.752	2.911	105	356	-0.289	-0.224	0.620
sonet23v4	1.407	1.366	79	181	-0.030	-0.029	0.550
sonet24v5	4.070	3.914	21	212	-0.040	-0.038	0.897
sonet25v6	5.161	4.812	10	45	-0.072	-0.068	0.762
sonetgr17	2.252	2.602	400	1247	0.134	0.134	0.722
space25	∞	∞	154	143	0.000	0.000	-0.071
spectra2	0.000	0.000	8	8	1.000	0.000	0.000
squff010-025	0.000	0.000	71985	75945	0.692	0.000	0.000
squff010-040	0.000	0.000	18478	20101	0.529	0.000	0.000
squff010-080	0.000	0.000	4509	8339	0.568	-0.000	0.000
squff010-080persp	0.000	0.000	6	6	1.000	0.000	0.000
squff015-060	0.000	0.000	7372	10223	0.608	-0.000	0.000
squff015-060persp	0.000	0.000	6	6	1.000	0.000	0.000
squff015-080	0.000	0.001	3475	6667	1.000	0.993	0.976
squff020-040	0.000	0.000	8358	10679	0.570	0.000	0.000
squff020-050	0.000	0.000	4094	8025	0.365	-0.000	0.000
squff020-150	0.014	0.014	9	7	0.000	0.000	-0.222
squff020-150persp	0.000	0.000	16	16	1.000	0.000	0.000
squff025-025	0.000	0.000	15093	11992	0.997	-0.000	-0.000
squff025-025persp	0.000	0.000	12	12	1.000	0.000	0.000
squff025-030	0.000	0.000	5523	14798	1.000	0.000	0.000
squff025-030persp	0.000	0.000	6	6	1.000	0.000	0.000
squff025-040	0.000	0.000	6438	7860	0.519	0.000	0.000
squff025-040persp	0.000	0.000	12	12	1.000	0.000	0.000
squff030-100	0.000	0.000	1291	1402	0.289	0.000	0.000
squff040-080	0.000	0.001	1034	1477	1.000	0.983	0.983

Continued on next page

Name	Gap Ours	Gap Base	Nodes Ours	Nodes Base	Reward	Utility	Utility/Node
squff040-080persp	0.000	0.000	8	8	1.000	0.000	0.000
sssd08-04persp	0.000	0.000	20080	17359	1.000	0.000	0.000
sssd12-05persp	0.131	0.133	63030	73358	0.016	0.016	0.154
sssd15-04persp	0.188	0.181	76121	77773	-0.041	-0.039	-0.018
sssd15-06persp	0.285	0.260	43387	47623	-0.095	-0.087	0.002
sssd15-08persp	0.235	0.234	30374	41340	-0.005	-0.005	0.261
sssd16-07persp	0.232	0.214	41858	46101	-0.086	-0.079	0.014
sssd18-06persp	0.200	0.188	40346	48551	-0.063	-0.059	0.117
sssd18-08persp	0.383	0.372	31676	41841	-0.028	-0.027	0.221
sssd20-04persp	0.202	0.202	63012	69887	0.002	0.002	0.100
sssd20-08persp	0.202	0.195	27951	34670	-0.036	-0.035	0.164
sssd22-08persp	0.228	0.212	31593	33795	-0.077	-0.071	-0.007
sssd25-08persp	0.178	0.172	27400	33837	-0.038	-0.037	0.159
st_bsj2	0.000	0.000	17	15	1.000	0.000	0.000
st_e05	0.000	0.000	59	75	1.000	0.000	0.000
st_e24	0.000	0.000	7	7	1.000	0.000	0.000
st_e25	0.000	0.000	15	15	1.000	0.000	0.000
st_e30	0.000	0.000	47	61	1.000	0.000	0.000
st_e31	0.000	0.000	593	490	1.000	0.000	0.000
st_fp7a	0.000	0.000	297	345	1.000	0.000	0.000
st_fp7b	0.000	0.000	349	341	1.000	0.000	0.000
st_fp7c	0.000	0.000	253	449	1.000	0.000	0.000
st_fp7d	0.000	0.000	277	355	1.000	0.000	0.000
st_fp7e	0.000	0.000	1605	1831	1.000	0.000	0.000
st_fp8	0.000	0.000	69	63	1.000	0.000	0.000
st_gimp_ss1	0.000	0.000	23	25	1.000	0.000	0.000
st_ht	0.000	0.000	13	11	1.000	0.000	0.000
st_iqpbk1	0.000	0.000	37	37	1.000	0.000	0.000
st_iqpbk2	0.000	0.000	39	37	1.000	0.000	0.000
st_jcbpaf2	0.000	0.000	9	13	1.000	0.000	0.000
st_m1	0.000	0.000	783	383	1.000	0.000	0.000
st_m2	0.000	0.000	637	619	1.000	0.000	0.000
st_pan1	0.000	0.000	11	11	1.000	0.000	0.000
st_ph11	0.000	0.000	11	11	1.000	0.000	0.000
st_ph12	0.000	0.000	13	13	1.000	0.000	0.000
st_ph13	0.000	0.000	9	9	1.000	0.000	0.000
st_qpc-m1	0.000	0.000	15	17	1.000	0.000	0.000
st_qpc-m3a	0.000	0.000	1269	1291	1.000	0.000	0.000
st_qpk1	0.000	0.000	7	7	1.000	0.000	0.000
st_qpk2	0.000	0.000	27	27	1.000	0.000	0.000
st_qpk3	0.000	0.000	137	133	1.000	0.000	0.000
st_rv1	0.000	0.000	107	81	1.000	0.000	0.000
st_rv2	0.000	0.000	133	119	1.000	0.000	0.000
st_rv3	0.000	0.000	511	629	1.000	0.000	0.000
st_rv7	0.000	0.000	1143	1153	1.000	0.000	0.000
st_rv8	0.000	0.000	1047	1269	1.000	0.000	0.000
st_rv9	0.000	0.000	3349	1875	1.000	0.000	0.000
st_testgr1	0.000	0.000	38	21	1.000	0.000	0.000
st_z	0.000	0.000	9	9	1.000	0.000	0.000
supplychain	0.000	0.000	119	95	1.000	0.000	0.000
tln12	0.295	0.217	20517	22942	-0.362	-0.266	-0.179
tln4	0.000	0.000	13	25	1.000	0.000	0.000
tln6	0.000	0.000	40	38	1.000	0.000	0.000
tln7	0.075	0.121	52425	60523	0.375	0.375	0.457
toroidal3g7_6666	0.200	0.117	51	213	-0.706	-0.414	0.592
tricp	∞	∞	275	356	0.000	0.000	0.228
util	0.000	0.000	48	38	1.000	0.000	0.000
wastewater02m1	0.000	0.000	43	43	1.000	0.000	0.000
wastewater02m2	0.000	0.000	35	31	1.000	0.000	0.000
wastewater04m1	0.000	0.000	117	81	1.000	0.000	0.000
wastewater04m2	0.000	0.000	25	25	1.000	0.000	0.000
wastewater05m1	0.000	0.000	2561	3047	1.000	0.000	0.000
wastewater05m2	0.000	0.000	4068	7429	1.000	0.000	0.000
wastewater11m1	0.116	0.131	40219	43385	0.113	0.113	0.177
wastewater11m2	0.385	0.431	15161	15304	0.106	0.106	0.114
wastewater12m1	0.099	0.045	23070	28082	-1.000	-0.541	-0.440
wastewater12m2	0.460	0.654	7232	7822	0.296	0.296	0.349
wastewater13m1	0.446	0.370	12150	16381	-0.207	-0.171	0.105
wastewater13m2	0.538	0.538	6204	6129	0.000	0.000	-0.012
wastewater14m1	0.151	0.122	38064	42510	-0.236	-0.191	-0.096
wastewater14m2	0.191	0.209	11743	13355	0.084	0.084	0.194
wastewater15m1	0.000	0.000	7735	8130	1.000	0.000	0.000
wastewater15m2	0.000	0.000	54228	59163	0.982	-0.000	-0.000
watercontamination0303	0.000	0.000	9	9	1.000	0.000	0.000
watercontamination0303r	∞	∞	22	37	0.000	0.000	0.405
waterund01	0.000	0.000	49001	57176	-0.022	-0.021	0.056
waterund08	0.000	0.000	38355	41489	0.335	0.083	0.003

Continued on next page

Name	Gap Ours	Gap Base	Nodes Ours	Nodes Base	Reward	Utility	Utility/Node
waterund11	0.001	0.001	35021	40695	-0.736	-0.420	-0.241
waterund14	0.009	0.009	9789	10684	-0.012	-0.012	0.072
waterund17	0.001	0.001	35708	36527	0.549	0.545	0.436
waterund18	0.001	0.001	34080	36286	0.049	0.048	0.085
waterund22	0.016	0.017	10195	10702	0.016	0.016	0.062
waterund25	0.080	0.094	11100	10382	0.154	0.153	0.095
waterund27	0.089	0.089	2253	2835	0.001	0.001	0.206
waterund28	0.080	0.080	18	17	0.000	0.000	-0.056
waterund36	0.100	0.082	1841	2443	-0.217	-0.178	0.083
Mean	—	—	6315	7463	0.487	0.000	0.114

J Alternative value function estimation

Benchmark	Reward	Win-rate	geo-mean Ours	geo-mean SCIP
TSPLIB (Reinelt, 1991)	0.150	0.68	0.86	0.957
UFLP (Kochetov & Ivanenko, 2005)	-0.071	0.39	0.569	0.552
MINLPLib (Bussieck et al., 2003)	0.497	0.84	32.5	31.185
MIPLIB (Gleixner et al., 2021)	0.038	0.61	789.31	848.628
TSPLIB@5min	0.173	0.63	1.73	2.000
MINLPLib@5min	0.507	0.82	18.04	20.460
MIPLIB@5min	0.282	0.77	44.892	106.400

We compare a different value function $V(s)$ parametrization, which can be interpreted as the value function as on-policy q-values $V(s) = \int \pi(a|s)Q(s, a)da$ and the fact that our actions correspond to individual nodes:

$$Q(n|s) = \frac{\tilde{Q}(n|s)}{|P(r, n)|} \quad (18)$$

$$\tilde{Q}(n|s) = \tilde{Q}(\text{left}|s) + \tilde{Q}(\text{right}|s) + q(h_K(n)|s) \quad (19)$$

$$V(s) = \sum_{\forall n \in \mathcal{C}} \tilde{Q}(n)\pi(n|s)dn \quad (20)$$

where $q(h_n)$ are the learned per-node estimator, \tilde{Q} the unnormalized Q-value, and \mathcal{C} is the set of open nodes as proposed by the branch-and-bound method. The advantage of this interpretation is that it allows one to interpret the path estimates \tilde{Q} as the on-policy q-values for each path. Having access to the q-values may be necessary for different actor-critic methods or the use of Deep Q-learning (Mnih et al., 2013).

K Pseudocode

Algorithm 1 Pseudocode for node selection using our policy

- 1: **procedure** NODE_SELECTOR
- 2: Apply message passing over tree T using Eq. 7
- 3: Compute root-to-leaf paths using Eq. 8
- 4: Compute policy π over selectable leaves using Eq. 9 \triangleright The value-function is only needed for training
- 5: Sample selected node $n \sim \pi$
- 6: run SCIP on n to get new children c_1, c_2
- 7: append c_1 and c_2 as children to n in tree T
- 8: (if necessary) prune T according to SCIP pruning rules

In our case, we set $N_{iter} = 16$, $K = 128$, and $\varepsilon = 0.1$, and the weight of the entropy regularization $\lambda_{ent} = 0.01$. In general, the policy improvement is the original PPO loss proposed in (Schulman et al., 2017), combined with implementation improvements provided in (Huang et al., 2021; 2022).

Algorithm 2 Pseudocode for training our policy

- 1: **procedure** POLICY_EVALUATION(π ,)
 - 2: sample random instance according to Section 4.4
 - 3: Solve using SCIP for 45s and node selector Alg. 2, record all trees $\{T_i\}_0^N$, selected nodes $\{a_i\}_0^N$, and final optimality gap
 - 4: Solve using SCIP for 45s without our node selector and record the final gap
 - 5: compute the reward r using Eq. 6
 - 6: compute the returns $R(s_t) = \gamma^{N-t}r$
 - 7: Compute Advantage $\{\hat{A}_i\}_0^N$ using GAE (Schulman et al., 2015) for all $\{T_i\}_0^N$ using value from Eq. 12.
 - return** $\{T_i\}_0^N, \{a_i\}_0^N, \{\hat{A}_i\}_0^N, R(s_t)$

 - 8: **procedure** POLICY_IMPROVEMENT (SCHULMAN ET AL., 2017)($\pi, \{T_i\}_0^N, \{a_i\}_0^N, \{\hat{A}_i\}_0^N, R(s_t)$)
 - 9: copy policy function π to π_{old}
 - 10: copy value function V to V_{old}
 - 11: **for** iteration= $i \dots N_{\text{iter}}$ **do**
 - 12: Optimize PPO-clip loss

$$L_t(\pi) = \min \left(\frac{\pi(a_i|T_i)}{\pi_{\text{old}}(a_i|T_i)} \hat{A}_i, \text{clip} \left(\frac{\pi(a_i|T_i)}{\pi_{\text{old}}(a_i|T_i)}, 1 - \varepsilon, 1 + \varepsilon \right) \hat{A}_i \right) + \lambda_{\text{ent}} H(\pi)$$
 - 13: using minibatch of size K sampled from the exploration data.
 - 14: Optimize Value estimate using clippe value-estimation

$$\begin{aligned} \text{mean} &= (R(s_t) - V(s_t))^2 \\ \text{clipped} &= V_{\text{old}}(s_t) + \text{clip}(V_{\text{old}}(s_t) - V(s_t), -\varepsilon, +\varepsilon) \\ L_v &= \max(\text{mean}, \text{clipped}) \end{aligned}$$
 - 15: using minibatch of size K sampled from the exploration data.
 - return** π, V

 - 16: **procedure** TRAIN(π, V)
 - 17: **for** Iterations **do**
 - 18: $\{T_i\}_0^N, \{a_i\}_0^N, \{\hat{A}_i\}_0^N, R(s_t) \leftarrow \text{Policy_Evaluation}(\pi)$
 - 19: $\pi, V \leftarrow \text{Policy_Improvement}(\{T_i\}_0^N, \{a_i\}_0^N, \{\hat{A}_i\}_0^N, R(s_t))$
 - return** π, V
-